

**Joint Pricing, Operational Planning and Routing Design
of a Fixed-Route Ride-sharing Service**

by

Wanqing Zhu

**A thesis submitted in partial fulfillment
of the requirements for the degree of
Master of Science in Engineering
(Industrial and Systems Engineering)
in the University of Michigan-Dearborn
2018**

Master's Thesis Committee:

**Assistant Professor Xi Chen, Chair
Assistant Professor Armagan Bayram
Associate Professor Jian Hu**

Acknowledgements

I wish to express my sincere gratitude to Dr. Xi Chen for her loving inspiration and timely guidance for this research. I am also very much thankful to the Ford Motor Company for their support on part of the research.

I also wish to thank my friend Meigui Yu for her help on the MNL data. And thanks to my family for their steady support and love.

Last but not least, I want to extend my appreciation to those who could not mentioned here but give me a lot of inspirations behind the curtain.

Table of Contents

Acknowledgements.....	ii
List of Tables	v
List of Figures.....	vi
Abstract.....	viii
Chapter 1: Introduction.....	1
Chapter 2: Joint Pricing and Operational Planning.....	2
2.1 Introduction.....	2
2.2 Literature Review.....	4
2.3 Model Formulation.....	6
2.3.1 The Raw Adoption Rate.....	8
2.3.2 Planning for the Price and Operations.....	10
2.4 Case Study.....	13
2.4.1 Datasets	13
2.4.2 Parameter Estimation	15
2.4.2.1 Travel Cost and Time.....	15
2.4.2.2 Total Travel Demand	20
2.4.2.3 Other Parameters.....	22
2.4.3 The Mode-Choice Model	22
2.5 Optimal Policy.....	26
2.6 Conclusion.....	33
Chapter 3: Fixed Route Design.....	34
3.1 Introduction.....	34
3.2 Literature Review	37
3.3 Model Formulation.....	39

3.4 Genetic Algorithm Based Approach	44
3.4.2 Initialization	46
3.4.3 Fitness value.....	47
3.4.4 Selection.....	47
3.4.5 Crossover.....	48
3.4.6 Mutation	49
3.5 Case Study.....	50
3.5.1 Problem Statement	50
3.5.2 Parameter Estimation	51
3.5.3 Result.....	52
3.5.4 Validation.....	55
3.6 Conclusion.....	58
Chapter 4: Conclusion and Discussion	59
Appendix.....	61
References.....	70

List of Tables

Table 2.1: Average Speed of Travel Modes	16
Table 2.2: Sample input data for transit time model.....	18
Table 2.3: Auto Mode Travel Cost	19
Table 2.4: Characteristics Selection.....	23
Table 2.5: 10-fold cross validation of mode-choice model	25
Table 2.6: Optimal pricing under current operational policy	27
Table 2.7: Jointly optimal pricing (linear price) and operational policy	27
Table 2.8: Jointly optimal pricing (flat rate only) and operational policy	28
Table 2.9: Estimate adoption rate of travel modes	32
Table 3.1: Parameters Definition	40
Table 3.2: Procedure for the Proposed GA Approach	45
Table 3.3: Simple random crossover procedure	48
Table 3.4: Simple random mutation procedure.....	49
Table 3.5: Computational results for parameter settings	52
Table 3.6: Results of validation on sample size of 20	55
Table 3.7: Results of validation on sample size of 30 for 2 routes	57

List of Figure

Figure 2.1: Route of RS	14
Figure 2.2: Census tracts and origins/destinations considered for Manhattan.....	17
Figure 2.3: Summary of regression output for Transit Time model	19
Figure 2.4: Gravity Model Log-linear Regression.....	20
Figure 2.5: Total travel demand estimates between service regions (S1 to S18 represent the stations along the route).....	21
Figure 2.6: Mode-choice model regression output	24
Figure 2.7: Comparing profits.....	28
Figure 2.8: Comparing adoption rates	29
Figure 2.9: Trade-off between profit and adoption rate (at knowledge level 1).....	31
Figure 3.1: General Procedure of Genetic Algorithm (figure adapted from Tasan, & Gen 2012).....	44
Figure 3.2: Genetic representation of the routing design problem	46
Figure 3.3: Roulette Wheel Selection	48
Figure 3.4: Station distance.....	51
Figure 3.5: Potential demand in Manhattan	52
Figure 3.6: Best routing design generated by GA.....	54
Figure 3.7: GA convergence plot.....	54
Figure 3.8: Comparison plot between GA and MILP on 20 sample size	56
Figure 3.9: Comparison plot between GA and MILP on 30 sample size for 2 routes.....	58

A1: Best routing design generated by GA for parameter (500, 500).....	61
A2: GA Convergence Plot for parameter (500, 500).....	62
A3: Best routing design generated by GA for parameter (500, 1000).....	63
A4: GA convergence plot for parameter (500, 1000).....	63
A5: Best routing design generated by GA for parameter (500, 1500).....	64
A6: GA convergence plot for parameter (500, 1500).....	64
A7: Best routing design generated by GA for parameter (1000, 500).....	65
A8: GA convergence plot for parameter (1000, 500).....	65
A9: Best routing design generated by GA for parameter (1000, 1000).....	66
A10: GA convergence plot for parameter (1000, 1000).....	66
A11: Best routing design generated by GA for parameter (1000, 1500).....	67
A12: GA convergence plot for parameter (1000, 1500).....	67
A13: Best routing design generated by GA for parameter (1500, 500).....	68
A14: GA convergence plot for parameter (1500, 500).....	68
A15: Best routing design generated by GA for parameter (1500, 1000).....	69
A16: GA convergence plot for parameter (1500, 1000).....	69

Abstract

Fixed-route ride-sharing services are becoming increasingly popular among major metropolitan areas, e.g., Chariot, OurBus, Boxcar. Effective routing design and pricing and operational planning of these services are undeniably crucial in their profitability and survival. However, the effectiveness of existing approaches have been hindered by the accuracy in demand estimation. In this paper, we develop a demand model using the multinomial logit model. We also construct a nonlinear optimization model based on this demand model to jointly optimize price and operational decisions. Moreover, we develop a mixed integer linear optimization model to the routing design decision. And a genetic algorithm based approach is proposed to solve the optimization model. Two case studies based on a real world fixed-route ride-sharing service are presented to demonstrate how the proposed models are used to improve the profitability of the service respectively. We also show how this model can apply in settings where only limited public data are available to obtain effective estimation of demand and profit.

Chapter 1: Introduction

The rapid growth of the sharing economy has been witnessed around the world in recent years. That is, the economy is undergoing a paradigm shift away from single ownership and towards shared ownership of goods and services. Successes have been seen, for example, in businesses that share habitation (e.g., Airbnb), financial services (e.g., CrowdFunding), vehicles (e.g., Car2go, ZipCar), and other mobility solutions (e.g., Uber, Chariot). Among these sharing services, ride-sharing is a particularly popular category, as evidenced by the popularity of Uber Pool and Lyft Line. Ride-sharing refers to the sharing of partial or whole trips among multiple riders using the same vehicle. By having more people using one vehicle, the traveling cost of each person can be reduced while vehicle capacity utilization can be significantly improved. Moreover, reduction in air pollution and traffic congestion may also result due to a reduction in the number of vehicles per trip demand. There are number of ride sharing companies operating different modes of sharing. Large cities have seen the most successful implementations of such ride-sharing services due to the immense opportunities of common trip segments. Among ride-sharing services, the specific business models take several forms, including the door-to-door model (e.g., Uberpool and Lyft Line), the corner-to-corner model (e.g., Via) and the fixed-route model (e.g., OurBus, Chariot, Boxcar). Both door-to-door service and corner-to-corner service are using real-time demand dynamically designing the route for every single ride. On the contrary, the fixed-route service is using the predicted demand and the predefined route for all rides.

The focus of this thesis is on fixed-route ride-sharing services, in which shuttles operate on fixed routes with predetermined stations. Customers of the service send request in advance to reserve a seat and then walk to and wait at a station by the scheduled time for their pick-up. Customers are charged a lower price than door-to-door ride-sharing service, while incurring longer travel times due to walking and waiting. Fixed-route ride-sharing services predominantly aim at serving commuters for completing trips to and from work. Comparing to traditional public transit, the fixed-route ride-sharing services have higher flexibility in route selection, provide better service (e.g., guaranteed seat and the on-board WIFI) and smart capabilities (e.g., real-time tracking of vehicles). Another critical difference between these fixed-route ride-sharing services and public transit is that these services are often provided by privately owned companies to whom profitability is a main concern. As a result, pricing is clearly a crucial decision for these services. In addition to price, how the service is operated can also have a significant effect on its profitability and market share. Moreover, the routing design based on the predicted travel demand also plays an important role by attracting more demands. For example, for a given customer, an affordable service with stations within close proximity would be most attractive, whereas an expensive service whose stations are far away would unlikely be a good choice. Therefore, paying more attention on the pricing and operation decisions as well as the routing design are more vital to the private ride-sharing company.

Chapter 2: Joint Pricing and Operational Planning

This chapter is organized as follows. Section 1 is the introduction to the joint price and operational planning for a ride-sharing service. Section 2 offers a review of related literature. Section 3 describes the model setup and formulates the joint pricing and operational planning problem as a nonlinear optimization problem. And section 4 provides a case study based on a real world fixed-route ride-sharing service, in which NYC commuter mode-choice are fitted using real data and the joint optimization problem proposed in Section 3 is solved. Section 5 offers concluding remarks.

2.1 Introduction

Pricing and operational planning are influenced by the potential demand of the ride-sharing service. There are two different aspects affect the potential demand of a service: internal and external. The internal factors are related to the ride-sharing service itself, such as: route design, station selection. External factors are related to the outside environment, for example, competitors and the demographic information of the service area. To reduce the effect of the internal factors, predetermined route and demand are used for the analysis of price and operation. On the other hand, to reduce the effect of external factors, a set of alternative competitors are predefined in the market. Different combinations of the pricing and operational policies can result to different profit. By maximizing the daily profit of the service, the optimal combination is obtained. Despite the importance of pricing and operational decisions, they have not been

adequately address primarily due to the difficulty to predict demand. This is due to several reasons. First, there is a lack of demand data of fixed-route ride-sharing and similar services. Most fixed-route ride-sharing services are relatively recent startups where systematic data collection have not been developed. Traditional transit services rarely vary their prices, resulting in particularly limited data points. In addition, customers may be reluctant to provide personal information due to privacy concerns. Second, as transportation systems become growing complex, there are many alternatives that compete for the demand of commuters. Third, the demand is affected by complex factors such as personal preference. For example, the attractiveness of an affordable service that requires significant amount of walking largely depends on the sensitivity of the customer towards cost versus time. In pricing and operational planning section, we develop a method using multinomial logit regression for the optimal pricing and operational planning of a fixed-route ride-sharing service that addresses the above challenges. Our contributions are as follows. First, we develop a demand model that incorporates concerns about cost, time, customer heterogeneity, and competing transportation alternatives. Using publicly available data, we show that this demand model is able to effectively predict customer mode choice and hence demand. Second, we develop an optimization model for jointly optimizing profit, fleet size and shuttle frequency based on the proposed demand model. Third, a case study of a real world fixed-route ride-sharing service is provided to demonstrate how the proposed models are used to improve the profitability of this service. Fourth, using the case study, we derive several interesting insights pertaining to the fixed-route ride-sharing service in New York City (NYC). For example, we find that introducing a per-distance rate has limited effect on the profitability of the service, and that the introduction of this service is predicted to be predominately divert customers from those who either take transit or walk to commute.

2.2 Literature Review

This work is related to the literature on the pricing of transportation services. As public transportation usually employs a flat rate, the majority of this literature has focused to the pricing of taxi services. Douglas (1972) develops an aggregate model with a constant fare per unit time and per unit travel distance to optimize the vacancy rate for the taxicab industry. However, Douglas (1972) does account for spatial effect on demand. This aggregate pricing model is widely used in later papers such as De Vany (1975), Arnott (1996) and Chang & Chu (2009). Arnott (1996) provides a dispatching model for taxis to reduce the subsidization for the taxicab industry, where he considers a space (a 2 dimensional city) within which taxis are randomly and uniformly distributed for implementation. Chang & Chu (2009) solve for the welfare-maximizing price for cruising taxi market, where the demand is assumed to be a log-linear function of price and average waiting time. Our work contributes to this literature by developing a new approach for estimating demand and an optimization program based on this demand model for jointly optimizing price as well as operational policies. Unlike the above literature, the demand estimation method in this work is based on real mode-choice decisions rather than a stylized demand function form. We also account for the effect of accessibility of the route in the demand function, which is not considered in taxi pricing since taxis provide door-to-door service. Moreover, our objective is to maximize the total operational profit, which differs from the typical objective of taxi fare optimization of maximizing the social willingness-to-pay.

The operational decisions considered in this paper include shuttle frequency, which has been studied in the literature on transit route configuration. This literature considers decisions include selection/improvement of routes as well as the optimal transit frequency, see for example Lampkin & Saalmans (1967), Silman et al. (1974), Marwah et al. (1984), Soehodho & Nahry (1998)

and Lee & Vuchic (2005). Within this literature, few have considered the joint optimization of both price and frequency of transit services, with Delle Site & Filippi (1998) and Chien & Spacovic (2001) being exceptions. However, they assume constant elasticity demand functions and do not provide methods for the calibration demand elasticity.

A key element of this work is the modeling of demand of the ridesharing service based on travel mode-choice decisions of customers. The literature on travel mode choice is extensive and we review some of the most relevant ones below. Deneubourg et al. (1979) develop a dynamic model to study the effect of behavioral fluctuations on the competing modes of automobile and public transportation. However, they do not consider the cost or service region of the transportation modes, or model the specific choice process. Much of the later literature use multinomial logit (MNL) model to model the decision making process, see for example Swait & Ben-Akiva (1987); Cervero & Kockelman (1997); Cervero (2002); Miller et al. (2005); Frank et al. (2008). Cervero & Kockelman (1997) introduce 3Ds: density, diversity and the design into the MNL model, and found them to be significant in mode-choice decisions. Cervero (2002) performs a model comparison between the original model and an expanded model with land-use and socio-economic variables based on a dataset based in Montgomery County, Maryland. Koppelman & Bhat (2006) introduce mode-choice modeling using multinomial and nested logit models in a report to the U.S Department of Transportation. They also carry out a micro-simulation on the SF bay area to validate the mode- choice model. Using a public transportation survey in Chicago, Javanmardi et al. (2015) conclude that individual and household socio-demographic, transit availability and vehicle availability play an important role in the modeling process. Consistent with this literature, we use the MNL model for mode-choice decisions, and consider all factors mentioned in the above paper including land- use, socio-economy and demographic factors. Using NYC RHTS and other

data, we fit a MNL model that can be used to predict NYC commuters' mode-choice decisions using only information of their origins and destinations. In contrast to the above literature which focuses on fitting the mode-choice model, we utilize the fitted model to simulate the demand of a fixed-route ridesharing service for inputting in pricing optimization.

Finally, this research is also related to the increasing literature on operational decisions in the sharing economy. For example, He et al. (2017) study the service region design problem for a one-way electric vehicle sharing system. They develop an adoption rate model and compute the profit using queueing theory. Furthermore, as the customers' requirements of real-time share increasing, the dynamic matching between vehicles and customers has received increasing attention from the operations management community, e.g., Agatz et al. (2012). This work contributes to this literature by studying the joint pricing and operational decisions of a fixed-route ride sharing system.

2.3 Model Formulation

Without loss of generality, we consider a fixed-route ride-sharing service provider who operates a one-way route, which we denote as RS. However, this assumption can be easily extended to two-way service, which is omitted for notational brevity. The set of stations is denoted as $S = \{1, 2, \dots, s\}$. For any $k \in \{1, 2, \dots, s\}$, service zone centered at station k is the region in which each point is located more than γ (in Manhattan distance) away from station k , denoted as $A(k)$. For example, the maximum distance that residents are willing to walk is considered as the radius of the service region of the service provider's stations. We denote the origin of a customer i as o_i and his/her destination as d_i . The origin station for customer i is denoted as o_i and the destination station is denoted as d_i . For simplicity, we discretize each service region into evenly

spaced (in Manhattan distance) Q points, and assume that the origins and destinations of customers are uniformly distributed among these Q points. Figure 3.1 illustrates this discretization in an example with $Q = 25$, where the star and dots represent the locations of the station and possible origin/destination of customers respectively and the grid represent the road directions. That is, if $o_i = k$ ($d_i = k$), the customer i 's origin (destination) locates at any point within the service region $A(k)$ with equal probability of 1. In addition to origin and destination, other characteristics of customer i (e.g., demographics, Q income) is summarized in an additional variable x_i . We define potential customers of RS as travelers whose origin is covered by the service region of a station of RS and whose destination is covered by the service region of a subsequent station of RS. We denote the probability density function of potential customers in service region $A(k)$ as $f_k(\cdot)$ and the set of possible values of x_i in $A(k)$ as X_k .

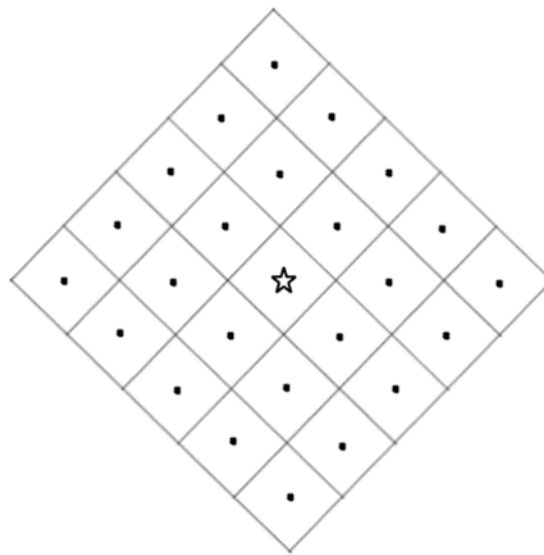


Figure 2.1 Discretization of possible origin/destination locations in a service region

2.3.1 The Raw Adoption Rate

The raw adoption rate of the ride-sharing service refers to the proportion of potential customers who prefer the service over other competing options. Note that the raw adoption rate differs from actual adoption rate of the service (see definition in Section 2.4) in that raw adoption rate does not factor in the capacity constraint of the service, and hence reflect solely customer preference. We estimate the raw adoption rate by modeling the travel mode-choice process for each potential customer whose origin and destination fall in the route's service regions using the classic Multinomial Logit (MNL) model. We define Φ as a set of all available travel modes and $RS \in \Phi$. The utility a customer i derives from choosing mode $\varphi \in \Phi$

$$U_{\varphi}(x_i, c_i^{\varphi}, t_i^{\varphi}) = V_{\varphi}(x_i, c_i^{\varphi}, t_i^{\varphi}) + \varepsilon_i^{\varphi}, \quad (2.1)$$

where c_i^{φ} is customer i 's cost of travel associated with model φ , and t_i^{φ} is customer i 's time of travel associated with model φ . $V_{\varphi}(x_i, c_i^{\varphi}, t_i^{\varphi})$ is the deterministic part of the customer's utility, which depends on cost of travel, time of travel, as well as customer i 's personal characteristics. ε_i^{φ} represents the random component of the utility function and is assumed to follow an extremely value distribution. We note that c_i^{φ} is a known fixed number once the origin and destination of the customer is known. It is also important to highlight that t_i^{φ} consists of not only the time of travel spent on the vehicle (denoted as $t_i^{\varphi,IV}$), but also walking time to and from the corresponding travel i mode for its access, denoted as $t_i^{\varphi,WT}$ and $t_i^{\varphi,WF}$ respectively. That is,

$$t_i^{\varphi} = t_i^{\varphi,WT} + t_i^{\varphi,IV} + t_i^{\varphi,WF}. \quad (2.2)$$

As a result, customer i chooses RS as his/her mode of travel if and only if $U_{RS}(x_i, c_i^{RS}, t_i^{RS}) \geq \max_{\varphi \in \Phi\{RS\}} \{U_{\varphi}(x_i, c_i^{\varphi}, t_i^{\varphi})\}$. Note that this formulation applies to scenarios where one or more travel modes that are unavailable to the customer, in which case high values may be assigned to c_i^{φ} or t_i^{φ} , or both. Let δ_i be a binary decision variable indicating whether customer i chooses to ride with RS (i.e., $\delta_i = 1$) or not (i.e., $\delta_i = 0$). Therefore, the probability of customer choosing RS as his/her mode of travel (given the origin, destination and personal characteristics of the customer) is

$$P(\delta_i = 1 | o_i, d_i, x_i) = \frac{\exp(V_{RS}(x_i, c_i^{RS}, t_i^{RS}))}{\sum_{\varphi \in \Phi} \exp(V_{\varphi}(x_i, c_i^{\varphi}, t_i^{\varphi}))}, \quad (2.3)$$

where c_i^{φ} and t_i^{φ} ($\varphi \in \Phi$) are known constants corresponding respectively to the costs and times determined by the origin and destination of the customer.

From the perspective of the service provider, x_i , o_i and d_i are often not directly observable. To address this issue, we propose the following steps for estimating the raw adoption rate. It is worthwhile to note that δ_i depends on the cost and time of travel associated with each mode, which is in turn affected by the locations of the customer's origin and destination. For example, a customer is more likely to choose to ride with RS if the other travel modes between his/her origin and destination are costly, time-consuming, or inaccessible. Therefore, it is important to differentiate between the raw adoption rates between different origin-destination pairs. The probability of customer i who travels from region $A(k)$ to region $A(j)$ requesting a ride with RS can be derived as follows:

$$\begin{aligned}
P(\delta_i = 1|O_i = k, D_i = j) &= \sum_{o_i \in A(k)} \sum_{d_i \in A(j)} \int_{X_k} P_i(\delta_i = 1|o_i, d_i, x_i) P(o_i|O_i = k) P(d_i|D_i = j) f_k(x_i) dx_i \\
&= \sum_{o_i \in A(k)} \sum_{d_i \in A(j)} \int_{X_k} \frac{\exp(V_{RS}(x_i, c_i^{RS}, t_i^{RS}))}{\sum_{\varphi \in \Phi} \exp(V_{\varphi}(x_i, c_i^{\varphi}, t_i^{\varphi}))} \frac{1}{Q^2} f_k(x_i) dx_i;
\end{aligned} \tag{2.4}$$

where $P(o_i|O_i = k)$ ($P(d_i|D_i = j)$) is the probability that customer i 's trip starts from (ends at) o_i (d_i) given that the pick-up (drop-off) station is station k (j), and recall that $f_k(\cdot)$ is the probability density function of potential customers in service region $A(k)$ and X_k is the set of possible values of x_i in $A(k)$. This value can be seen as the raw adoption rate of RS among customers who travel from region $A(k)$ to region $A(j)$. In what follows, we denote $AR_{kj} = P(\delta_i = 1|O_i = k, D_i = j)$ for notational convenience.

Finally, let p_k^j denote the probability that the pick-up station of potential customer is station k and the drop-off station is station j , then the overall raw adoption rate of RS among all customers covered by its service regions can be calculated as

$$P(\delta_i = 1) = \sum_{k=1}^s \sum_{j=k+1}^s P(\delta_i = 1|O_i = k, D_i = j) p_k^j. \tag{2.5}$$

2.3.2 Planning for the Price and Operations

A well-designed pricing and operating policy allows the service provider to balance the desire to increase demand and revenue with the associated cost. On the one hand, it benefits the customers and increases demand if the service provider either increases the shuttle departure frequency on each route or lowers the price. On the other hand, a higher frequency or a lower price

may lead to lower profit margin. Therefore, it is important to assess whether increasing revenue or profit margin is more effective, and whether either objective should be achieved through changing price or operations, or both.

In this section, we develop an optimization model for jointly optimizing the price and operations, i.e., shuttle departure frequency, of the ride-sharing service. For ease of exposition, we consider a linear pricing rule

$$c_i^{RS} = c_1 d_{O_i D_i} + c_2, \quad (2.6)$$

where c_1 is rate per unit of distance traveled with RS (d_{xy} represents the distance between x and y), and c_2 is the flat rate charged per ride. Linear pricing is common in practice among various transportation modes used for commuting, e.g., public transit, taxi.

The operating cost consists of two components: a fixed cost per day per vehicle, denoted as F_f , and a variable cost dependent on the number of times each vehicle drives through the route, denoted as F_v . Examples of the fixed cost include vehicle rental, driver wage, insurance, parking, cleaning and maintenance and data fee. The variable cost includes for example fuel cost and hourly payments to drivers. Total operating time per day is denoted as T , and the total time for completing a trip and back to the starting station is TR . The fleet size is n . Shuttles depart every β minutes and the capacity of each shuttle is N . Overall customer travel demand (including all transportation modes) from service region of station k to station j per unit time is denoted as D_{kj} . The walking and driving speed are assumed to be constant and denoted as s_w and s_d , respectively. d_{kj} denotes the distances between stations k and j for simplification.

The service provider RS simultaneously chooses c_1 , c_2 , β and n to maximize its profit. Note that not all customer travel requests are guaranteed to be satisfied by RS due to its capacity limitation. To capture this consideration, we also introduce an intermediate decision variable y_{kj} to represent the expected number of requests from station k to station j that are fulfilled by RS. Hence, the optimization problem of RS can be formulated as

$$\max_{c_1, c_2, \beta, y_{kj}, n} \frac{T}{\beta} \left(\sum_{k=1}^s \sum_{j=k+1}^s (c_1 d_k^j + c_2) \times y_{kj} - F_v \right) - n F_f \quad (2.7)$$

$$s. t. \quad y_{kj} \leq \beta D_{kj} AR_{kj}, \quad for \ k = 1, \dots, s-1, j = k+1, \dots, s \quad (2.8)$$

$$\sum_{k \leq l, j > l} y_{kj} \leq N, \quad for \ k, l = 1, \dots, s-1, j = k+1, \dots, s \quad (2.9)$$

$$AR_{kj} = \sum_{o_i \in A(k)} \sum_{d_i \in A(j)} \int_{X_k} \frac{\exp \left(V_{RS} \left(x_i, c_1 d_k^j + c_2, \frac{d_{o_i k} + d_j}{s_w} + \frac{d_k^j}{s_d} \right) \right)}{\sum_{\varphi \in \Phi} \exp \left(V_{\varphi} \left(x_i, c_i^{\varphi}, t_i^{\varphi} \right) \right)} \frac{1}{Q^2} f_k(x_i) dx_i, \quad (2.10)$$

for $k = 1, \dots, s-1, j = k+1, \dots, s$

$$\beta \geq \frac{T_R}{n}, \quad (2.11)$$

$$c_1, c_2 \geq 0 \quad (2.12)$$

The first constraint guarantees that the number of fulfilled trips between stations k and j does not exceed the total number of trips requested by customers. The second constraint ensures that the capacity constraint of each shuttle is not violated at each station. The third constraint is derived from the adoption rate model illustrated in Section 3.1, relating the price of service to the adoption rate of the service among potential customers traveling from $A(k)$ to $A(j)$. The fourth

constraint assures that the shuttle departure interval is feasible given the shuttle fleet size, i.e., the shuttles have sufficient time to return to the starting station after completing the route in order to follow the schedule.

2.4 Case Study

In this section, we present a case study based on a real world fixed-route ride-sharing service to demonstrate how the model from Section 3 can be applied. We continue to refer to this service as RS. The route analyzed in the following operates in New York City (NYC) and has 18 stations; see Figure 4.1 for an illustration. Customers can book a ride by specifying pick-up and drop-off stations 10 minutes before departure time during the operating hours of 7:00 AM - 10:30 AM and 4:00 PM - 7:30 PM on weekdays. Shuttles depart every 10-15 minutes on this route. The current pricing policy is a flat rate of \$4/ride.

2.4.1 Datasets

Several datasets are used in this case study. First, the 2010/2011 Regional Household Travel Survey (RHTS) data is used to model the consumer mode-choice model. RHTS data is collected by the New York Metropolitan transportation council and provides travel statistics from fall of 2010 to fall of 2011 in New York, New Jersey and Connecticut. Nearly 19,000 households across 28 counties participated in the survey. Travel information including trip purpose, trip time and distance, and activities during the trip. Other geographic information and demographic information are also recorded using self-reported data and GPS data. For majority of our analysis (except for estimating average speed of transportation), RHTS data related to commuter trips within and between Manhattan and Brooklyn were selected because the target customers of RS are

residence and workplace State, County and Census Tract. The 2010 American Census Data and the MTA New York City Travel Survey Data are used to estimate the distribution of the demographic and socioeconomic factors of potential customers. The research team is also provided with the operational cost data of RS.

The authors have also collected from various other data sources to supplement the above datasets, such as using the Google Maps API, the details of which will be discussed in the following subsections.

2.4.2 Parameter Estimation

In this section, we estimated the input parameters for the model described in Section 3 for optimizing the price and operations of RS.

2.4.2.1 Travel Cost and Time

In order to estimate customer's adoption rate using the model described in Section 3.1, we need to estimate the cost and time associated with all modes considered. For the chosen mode of each trip, this information is readily available in the RHTS data. However, the cost and time associated with other (not chosen) modes have to be estimated. We explain the methods for their estimation below.

We first compute the average speed for the three travel modes considered, by directly dividing trip distance used by a given mode recorded in RHTS data by its corresponding trip duration; see Table 4.1. All recorded trips are used to ensure a sufficient sample size and result reliability.

Table 2.1: Average Speed of Travel Modes

Alternatives	Transit	Auto	Walk
Avg. Speed (mi/min)	0.098	0.117	0.0325

Walk Time

Travel time using mode walk (Walk Time) is estimated directly using average walking speed:

$$Walk\ Time = \frac{Trip\ Distance}{0.0325mi/min}$$

Auto Time

Travel time using the auto mode is estimated as:

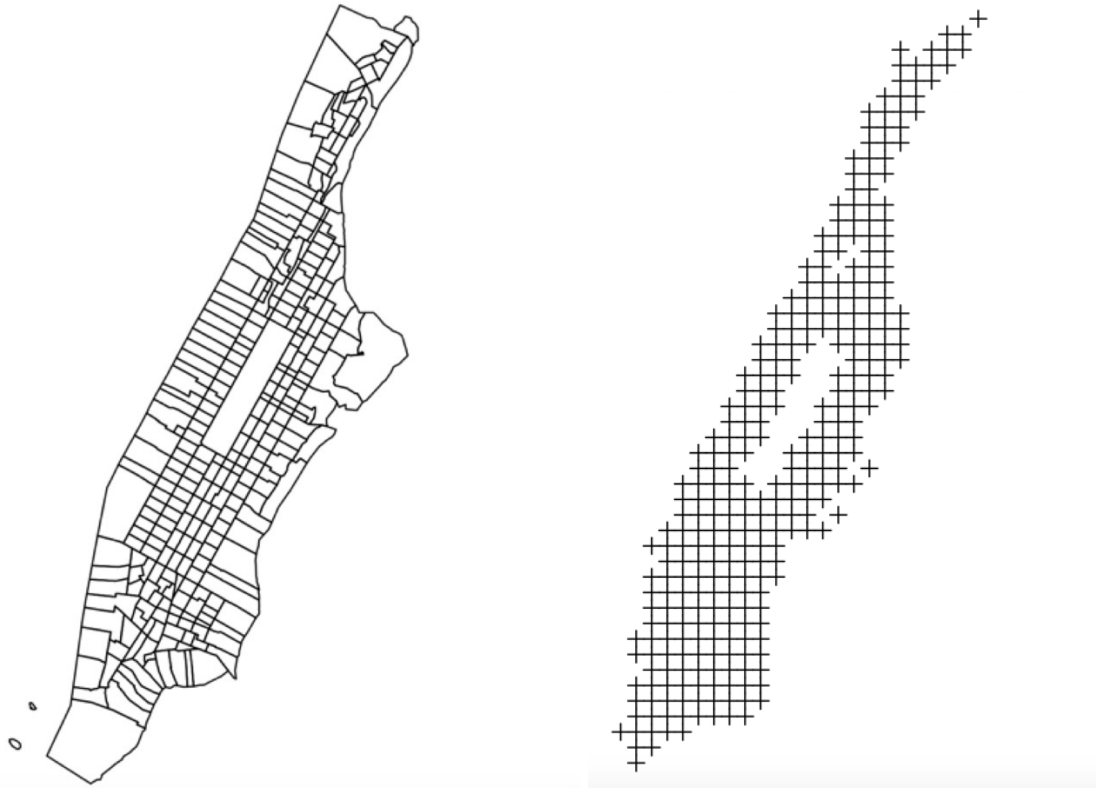
$$Auto\ Time = \frac{Trip\ Distance}{0.117mi/min} + Out\ of\ Vehicle\ Travel\ Time$$

where the Out of Vehicle Travel Time consists of the walking time to the parking lot and to the workplace, and is assumed to average 5 minutes.

Transit Time

Travel time using mode transit (Transit Time) is more variable and may be affected by number of factors, such as travel distance, time of the day, accessibility of transit stations and transit frequency. We postulate that the population and income level (of both origin and destination) are key indicators of socioeconomic characteristics of an area. For example, the higher the population, the more congestion there may be, while the more accessible transit may be. As a result, transit time may vary from census tract to census tract. To capture this feature, we use census tract as our lowest resolution for population and income, and then uniformly generate large number of possible origins or destinations using the Geographic package in R (points that fall in areas where

residence is impossible, e.g. central park, river, are eliminated). We note that only locations in Manhattan are considered for the purposed of estimating Transit Time, due to the lack of transit time data for trips originating/terminating in Brooklyn. Figure 2.2 illustrates Manhattan census tracts and uniformly generated origins or destinations considered.



(a). Manhattan census tracts

(b). Uniformly generated origin and destinations

Figure 2.2: Census tracts and origins/destinations considered for Manhattan

The Google Map Direction API is used to obtain the real transit travel times between any 2 points in Figure 2.2b. We collected times for trips during both rush hours and non-rush hours on weekdays. Weekend trips are not considered because RS does not operate on weekends. We also find the average income and population for the corresponding census tract of each point in Figure 2.2b. Some example data points are provided in Table 2.2.

Table 2.2: Sample input data for transit time model

time	distance	ini_inc	des_inc	rush
1597	1.523440818	221457	285447	1
1257	1.277037684	221457	225338	1
717	0.791910883	221457	251818	1
540	0.559881348	221457	251818	1
647	0.353942159	221457	160140	1
462	0.250093244	221457	160140	1
...

The transit travel time is fitted using multiple linear regression in R software. The output is summarized in Figures 2.3. We can see that the coefficients for all four independent variables, i.e., *distance* (trip distance), *ini_inc* (average income of the origin census tract), *des_inc* (average income of the destination census tract) and *rush* (a dummy variable indicating whether the trip is taken during rush hours), are significant. The R-squared value of the model is 0.909, which indicates a good fit. The regression results therefore suggest a transit time model given as follows

$$\begin{aligned}
 \text{Transit Time} = & 322.1 \times \text{distance} + 1.702 \times 10^{-3} \times \text{ini}_{inc} + 1.896 \times 10^{-3} \\
 & \times \text{des}_{inc} + 176.2 \times \text{rush},
 \end{aligned}
 \tag{2.13}$$

```

> lmodel=lm(time~0+distance+ini_inc+des_inc+rush)
> summary(lmodel)

Call:
lm(formula = time ~ 0 + distance + ini_inc + des_inc + rush)

Residuals:
    Min       1Q   Median       3Q      Max
-2364.2  -302.8    78.0   483.6  4716.6

Coefficients:
            Estimate Std. Error t value Pr(>|t|)
distance  3.221e+02   4.624e-01   696.50  <2e-16 ***
ini_inc   1.702e-03   1.416e-05   120.18  <2e-16 ***
des_inc   1.896e-03   1.416e-05   133.83  <2e-16 ***
rush     1.762e+02   2.753e+00    63.98  <2e-16 ***
---
Signif. codes:  0 '***' 0.001 '**' 0.01 '*' 0.05 '.' 0.1 ' ' 1

Residual standard error: 629.6 on 190340 degrees of freedom
Multiple R-squared:  0.909, Adjusted R-squared:  0.909
F-statistic: 4.752e+05 on 4 and 190340 DF, p-value: < 2.2e-16

```

Figure 2.3: Summary of regression output for Transit Time model

Travel Cost

The monetary cost of each travel mode considered is estimated as follows. The cost for walk is zero. For transit, we estimate the cost using the fare for a subway or local bus ride, which is a fixed flat rate of \$ 2.75/ride. For the auto mode, the cost estimate consists of three components: gas fee, parking fee, as well as a toll fee (source: NYC DOT) for passing the bridge if a customer traveling from Manhattan to Brooklyn or vice versa. The value of each auto mode cost component is provided in Table 4.3. For example, the cost of a trip from Manhattan to Brooklyn, is estimated as $0.15 \times distance + 9.5 \times parking\ time + 5.76$. Here, the parking time is estimated as the full-time working hours per day, i.e., 8 hours.

Table 2.3: Auto Mode Travel Cost

	Manhattan-Manhattan	Brooklyn- Brooklyn	Intra-Borough
Gas Fee (\$/mi)	0.15	0.15	0.15
Parking Fee (\$/day)	10	9	9.5
Toll Fee (\$/time)	0	0	5.76

2.4.2.2 Total Travel Demand

We first estimate the overall inter-census-tract travel demand based on the CTPP 2006-2010 Census Tract Flows (CTF) data of commuter trips. We use the flow between census tracts provided by CTF data to represent the total travel demand along RS's Route. For travel between census tract pairs missing in CTF data and intra-census-tract travel, we supplement the input with travel flow estimates using the gravity model (Anderson (2011)) as detailed below.

Based on the gravity model, we estimate the total travel demand between census tract i and census tract j to be:

$$T_{ij} = \beta_1 \frac{Pop_i Pop_j Inc_i^{\beta_2} Inc_j^{\beta_3}}{dist_{ij}^{\beta_4}} \quad (2.14)$$

where Pop_i (Pop_j) is the population of census tract i (j), Inc_i (Inc_j) is the average income in census tract i (j), and $dist_{ij}$ is the distance between the geometric centers of census tracts i and j . We then fit the above gravity model using the CTF data. Figure 2.4 summarizes the model fit output in R.

```
Call:
lm(formula = log(EST) ~ log(Hinc) + log(Winc) + log(Hpop) + log(Wpop) +
    log(distance), data = gravity)

Residuals:
    Min       1Q   Median       3Q      Max
-2.1416 -0.4898 -0.0113  0.4777  3.3889

Coefficients:
            Estimate Std. Error t value Pr(>|t|)
(Intercept)  -0.681387   0.061754  -11.03  <2e-16 ***
log(Hinc)     0.049692   0.004822   10.30  <2e-16 ***
log(Winc)     0.077059   0.003935   19.58  <2e-16 ***
log(Hpop)     0.344672   0.005303   65.00  <2e-16 ***
log(Wpop)    -0.055618   0.002960  -18.79  <2e-16 ***
log(distance) -0.059280   0.003462  -17.12  <2e-16 ***
---
Signif. codes:  0 '***' 0.001 '**' 0.01 '*' 0.05 '.' 0.1 ' ' 1

Residual standard error: 0.6873 on 59635 degrees of freedom
Multiple R-squared:  0.1086, Adjusted R-squared:  0.1085
F-statistic: 1453 on 5 and 59635 DF, p-value: < 2.2e-16
```

Figure 2.4: Gravity Model Log-linear Regression

Using the methods described above, we estimate the total potential travel demand for RS by assuming demand is evenly split between either direction in both mornings and afternoons. Final estimates of total demand between service regions along the Manhattan-to-Brooklyn and Brooklyn-to-Manhattan directions are provided in Figure 2.5a and Figure 2.5b, respectively. We can see that a significant portion of travel demand are for intra-census-tract travels, which is consistent with the observation of high proportion of walk mode in the RHTS survey.

Stations	s1	s2	s3	s4	s5	s6	s7	s8	s9	s10	s11	s12	s13	s14	s15	s16	s17	s18	
s1	10	4	4	4	5	4	4	10	4	4	4	4	4	4	4	4	4	4	4
s2	0	63	70	30	30	15	10	8	8	9	9	10	10	9	10	9	9	9	9
s3	0	0	173	60	10	35	9	10	9	10	10	10	10	10	10	10	10	10	10
s4	0	0	0	65	80	10	10	10	10	11	11	10	10	10	10	10	10	10	10
s5	0	0	0	0	20	4	4	4	4	5	5	5	5	5	5	5	5	5	5
s6	0	0	0	0	0	225	150	25	10	15	15	14	15	14	15	14	14	14	14
s7	0	0	0	0	0	0	260	80	13	14	14	14	14	14	14	14	14	14	13
s8	0	0	0	0	0	0	0	330	35	14	14	14	13	14	13	14	13	13	13
s9	0	0	0	0	0	0	0	0	245	15	15	14	15	14	14	14	14	14	14
s10	0	0	0	0	0	0	0	0	0	20	40	6	7	7	7	7	7	7	7
s11	0	0	0	0	0	0	0	0	0	0	20	6	7	7	7	7	7	7	7
s12	0	0	0	0	0	0	0	0	0	0	0	105	10	10	10	10	10	10	10
s13	0	0	0	0	0	0	0	0	0	0	0	0	58	7	7	10	10	10	7
s14	0	0	0	0	0	0	0	0	0	0	0	0	0	115	10	40	40	40	10
s15	0	0	0	0	0	0	0	0	0	0	0	0	0	0	95	9	9	9	15
s16	0	0	0	0	0	0	0	0	0	0	0	0	0	0	0	60	120	10	10
s17	0	0	0	0	0	0	0	0	0	0	0	0	0	0	0	0	60	10	10
s18	0	0	0	0	0	0	0	0	0	0	0	0	0	0	0	0	0	60	138

(a). Manhattan-to-Brooklyn Direction

Stations	s1	s2	s3	s4	s5	s6	s7	s8	s9	s10	s11	s12	s13	s14	s15	s16	s17	s18	
s1	10	0	0	0	0	0	0	0	0	0	0	0	0	0	0	0	0	0	0
s2	45	63	0	0	0	0	0	0	0	0	0	0	0	0	0	0	0	0	0
s3	11	25	173	0	0	0	0	0	0	0	0	0	0	0	0	0	0	0	0
s4	12	10	125	65	0	0	0	0	0	0	0	0	0	0	0	0	0	0	0
s5	5	10	5	5	20	0	0	0	0	0	0	0	0	0	0	0	0	0	0
s6	17	50	90	75	90	225	0	0	0	0	0	0	0	0	0	0	0	0	0
s7	120	85	90	155	145	45	260	0	0	0	0	0	0	0	0	0	0	0	0
s8	55	25	110	40	205	40	85	330	0	0	0	0	0	0	0	0	0	0	0
s9	160	30	135	120	115	75	55	45	245	0	0	0	0	0	0	0	0	0	0
s10	15	14	8	7	8	7	7	7	20	20	0	0	0	0	0	0	0	0	0
s11	15	7	8	7	8	7	7	7	20	40	20	0	0	0	0	0	0	0	0
s12	105	7	40	15	15	11	40	40	11	11	11	105	0	0	0	0	0	0	0
s13	10	12	25	20	30	20	8	8	8	8	8	7	58	0	0	0	0	0	0
s14	25	25	40	50	45	10	10	10	11	12	12	11	11	115	0	0	0	0	0
s15	25	10	11	11	15	10	10	20	10	10	10	9	10	9	95	0	0	0	0
s16	10	11	15	13	15	13	12	12	12	12	12	12	12	11	20	60	10	10	0
s17	10	13	15	13	15	13	12	12	12	12	12	12	12	11	20	120	60	10	0
s18	10	13	10	50	10	13	13	10	13	10	12	12	13	10	11	11	11	11	138

(a). Brooklyn-to-Manhattan Direction

Figure 2.5: Total travel demand estimates between service regions (S1 to S18 represent the stations along the route)

We assume that potential origins and destinations are uniformly distributed among 25 points within the service region of each station (see Figure 2.1 for an illustration). The radius of the service region of each station is assumed to be the maximum distance NYC residents are willing to walk, that is, 0.25 miles (Yang & Diez-Roux (2012)). Origins and destinations in areas

where two or more service regions overlap are assigned to the service region of their closest respective station. This is to ensure that no customer gets counted twice and that everyone takes the shuttle from the nearest station. Using the above method, we generate all potential origins and destinations for customers.

2.4.2.3 Other Parameters

Based on the station coordinates, the Manhattan distances between pairs of stations are calculated to represent the distances of travel between RS's stations. The RS shuttle travel time are estimated using the Google Maps API by treating the automobile travel time from one station to another as the corresponding RS shuttle travel time. Finally, we also recognize that a large portion of NYC residence do not own a car (77% according to StatsBee), making the auto mode infeasible for them. To factor in this consideration, we randomly select 77% of the potential trips and assign a very large cost to the auto mode for them, effectively excluding the auto mode from the available modes for these trips.

2.4.3 The Mode-Choice Model

We consider several demographic and socio-economic factors suggested by Javanmardi et al. (2015) in the initial model, which include age, income, gender, access to transit, vehicle ownership, employment, gross population density, land-use diversity. We also introduce dummy variables for whether the origin/destination is in Brooklyn or not. These factors are estimated based on the American Fact Finder Census 2010 (AFC) and the NYC Travel Survey Data (NTS). After initial model fit, we find that 6 out of 12 factors are insignificant and hence are dropped from the model. Table 2.4 summarizes the above results.

Table 2.4: Characteristics Selection

Demographics	Data Source	Significant? (Y/N)
Age	NTS	Y
Income	NTS	Y
Gender	NTS	Y
Origin Brooklyn	AFC	Y
Destination Brooklyn	AFC	Y
Access to Transit	AFC	N
Vehicle Ownership	AFC	Y
Full-time Employed	AFC	N
gross density of origin census tract	AFC	N
land-use diversity of origin census tract	AFC	N
gross density of destination census tract	AFC	N
land-use diversity of destination census tract	AFC	N


```

Call:
mlogit(formula = mode ~ cost + time | age + income + gender +
      obr + dbr + VEHNO, data = newdata, method = "nr", print.level = 0)

Frequencies of alternatives:
      auto transit  walk
0.18742 0.59669 0.21589

nr method
7 iterations, 0h:0m:0s
g'(-H)^-1g = 0.000838
successive function values within tolerance limits

Coefficients :
              Estimate Std. Error t-value Pr(>|t|)
transit:(intercept) 2.7147e-01 3.5480e-01  0.7651 0.4441909
walk:(intercept)    7.8443e-01 4.2274e-01  1.8556 0.0635122 .
cost                -2.1479e-01 2.3781e-02 -9.0320 < 2.2e-16 ***
time               -3.7087e-02 1.7583e-03 -21.0925 < 2.2e-16 ***
transit:age         1.9790e-03 5.0227e-03  0.3940 0.6935687
walk:age            -7.9584e-03 5.7012e-03 -1.3959 0.1627417
transit:income      4.0281e-06 1.5688e-06  2.5677 0.0102367 *
walk:income         9.0963e-07 1.8082e-06  0.5031 0.6149201
transit:gender      1.0902e-01 1.1530e-01  0.9456 0.3443676
walk:gender         1.8895e-02 1.3342e-01  0.1416 0.8873810
transit:obr         -5.5197e-01 1.5619e-01 -3.5340 0.0004094 ***
walk:obr            -5.5928e-01 2.6183e-01 -2.1360 0.0326779 *
transit:dbr         -7.3265e-01 1.5459e-01 -4.7394 2.144e-06 ***
walk:dbr            -5.3280e-01 2.6089e-01 -2.0422 0.0411297 *
transit:VEHNO      -1.0943e+00 7.1786e-02 -15.2441 < 2.2e-16 ***
walk:VEHNO         -7.8089e-01 7.9816e-02 -9.7836 < 2.2e-16 ***
---
Signif. codes:  0 '***' 0.001 '**' 0.01 '*' 0.05 '.' 0.1 ' ' 1

Log-Likelihood: -2063.8
McFadden R^2: 0.28283
Likelihood ratio test : chisq = 1627.8 (p.value = < 2.22e-16)

```

Figure 2.6: Mode-choice model regression output

After eliminating the insignificant characteristics, we consider trip-specific variables including time and cost, and personal characteristics including, age, income, gender, origin from Brooklyn, destination in Brooklyn and vehicle ownership when fitting the MNL model. Figure 2.6 summarizes the regression output in R. We find that cost and time are both highly significant in mode-choice decisions for all travel modes. As the cost and/or time of a mode increases, the probability of customers choosing the mode decreases. Number of vehicles in the household (VEHNO) is significant for both walk and transit. If the number of vehicles per household increases, a person in that household is more likely to choose auto rather than walk or transit. The origin and/or destination being in Brooklyn has a significant impact on mode choice, however,

it is more significant for choosing transit than choosing walk. Income is significant for choosing transit but not for choosing walk. Age and gender are not significant in all modes. The likelihood ratio test is significant at 99.9% confidence level, suggesting a reliable model.

We performed a 10-fold cross validation (randomly selecting 90% of the data as training data and using the rest 10% as the test data) to examine the prediction accuracy of the fitted mode-choice model. Table 2.5 summarizes the result. We can see that the prediction accuracy is reasonable overall (59.64-81.45%), and higher for Transit (66.67-91.86%) and Walk (65.79-80%) modes. Prediction accuracy for auto mode is less reliable, varying from 6.98% to 60.71%. This is a result of the small sample size of the auto mode (566 records out of 3020 in total). However, the target customer group of RS is commuters in NYC, whose main competition comes from traditional or new forms of public transit and walking. Therefore, the prediction accuracy of auto mode is expected to have limited effect on the analysis.

Table 2.5: 10-fold cross validation of mode-choice model

Predict Accuracy	Transit	Auto	Walk	Overall
1	84.48%	28.26%	80.00%	74.18%
2	84.15%	33.33%	74.47%	74.18%
3	88.65%	13.16%	69.23%	74.55%
4	84.21%	6.98%	67.21%	68.36%
5	84.12%	20.93%	79.03%	73.09%
6	66.67%	39.13%	65.79%	59.64%
7	89.36%	44.23%	78.05%	77.54%
8	91.86%	42.11%	76.92%	81.45%
9	82.35%	38.37%	75.34%	72.73%

10	83.22%	60.71%	68.75%	73.82%
----	--------	--------	--------	--------

2.5 Optimal Policy

In this section, we discuss the optimal pricing and operational policy for RS. Several competing travel modes are considered, including transit, auto, walk. In addition, we also consider another major competitor of RS — Via, which is another ride-sharing service provider offering corner-to-corner service for \$5 flat fee in NYC. Note that because the RHTS data does not contain ride-sharing modes, the utility function of the transit mode is used for both RS and Via due to the similarity between their services. We study three cases: (i) when RS chooses optimal prices only given the current operation policy of 10-minute departure intervals and fleet size of 7 (i.e., the smallest fleet size that enables 10-minute departure interval), (ii) when RS simultaneously chooses optimal prices and operational decisions; and (iii) when RS simultaneously chooses optimal prices and operational decisions and prices are flat rates only. For each case, we examine the performance of the optimal policy in terms of profit and average adoption rate (percentage of customers adopting RS’s service among those who know of RS) under varying customer knowledge levels, i.e., percentage of people who know about RS, of 10%, 20%, 50% and 100%.

Tables 2.6 - 2.8 present the optimal policy and performance for the three cases mentioned above. For example, in case (ii), when the knowledge level is 5%, the optimal price is a flat rate of \$4.7659 and a distance-based rate of \$ 1.5268 mi/min under the current departure interval. We can also see that the optimal prices do not vary in case (i). This is because in case (i) the shuttles depart so frequently that there are always excessive capacity.

Table 2.6: Optimal pricing under current operational policy

Knowledge	c_1 (\$/mi)	c_2 (\$)	β (min)	n	Average Adoption Rate	Profit (\$)
0.1	0.1661	5.2668	10	7	1.35%	-1322.1
0.2	0.1661	5.2668	10	7	2.71%	-977.1184
0.5	0.1661	5.2668	10	7	6.77%	57.7013
1	0.1661	5.2668	10	7	13.54%	1782.4

Table 2.7: Jointly optimal pricing (linear price) and operational policy

Knowledge	c_1 (\$/mi)	c_2 (\$)	β (min)	n	Average Adoption Rate	Profit (\$)
0.1	0.1887	5.2589	194.1266	1	1.45%	110.1669
0.2	0.1887	5.2589	97.0633	1	2.90%	453.1939
0.5	1.5268	4.7659	65	1	5.72%	1382.2
1	1.5268	4.7659	32.5	2	11.45%	2764.5

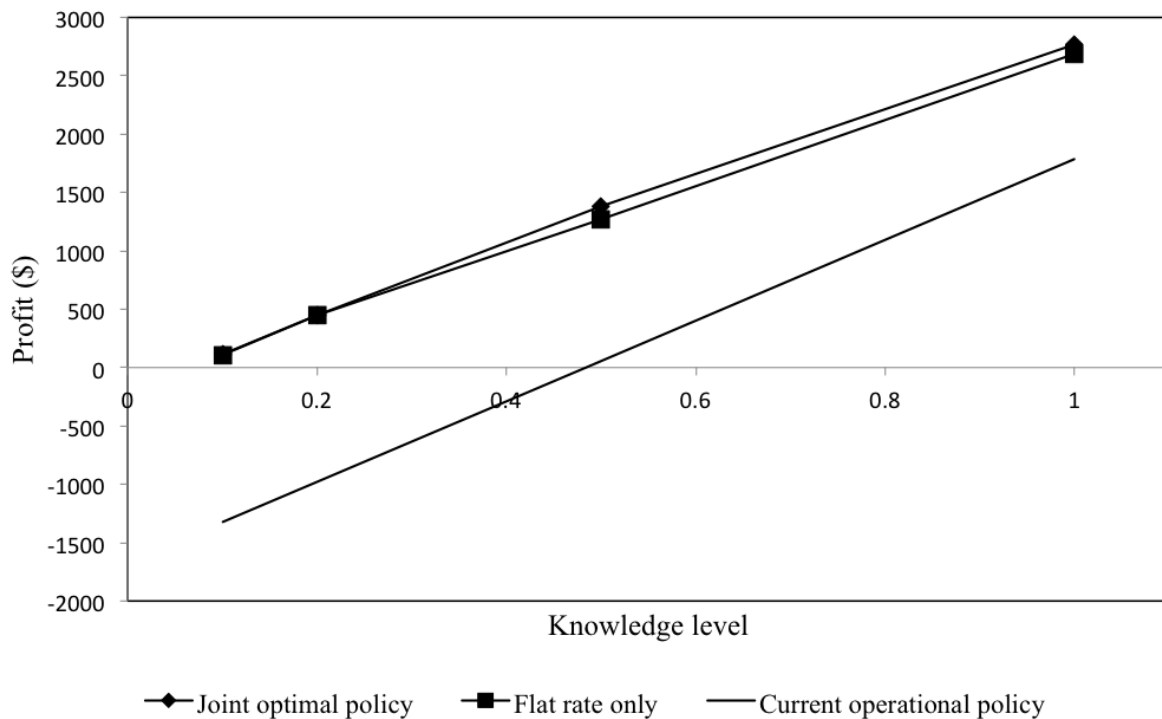


Figure 2.7: Comparing profits

Table 2.8: Jointly optimal pricing (flat rate only) and operational policy

Knowledge	c_1 (\$/mi)	c_2 (\$)	β (min)	n	Average Adoption Rate	Profit (\$)
0.1	0	5.5707	187.8345	1	1.44%	109.8949
0.2	0	5.5407	93.9173	1	2.89%	452.6498
0.5	0	8.5292	65	1	4.11%	1269.3
1	0	6.3472	21.6667	3	11.34%	2689.4

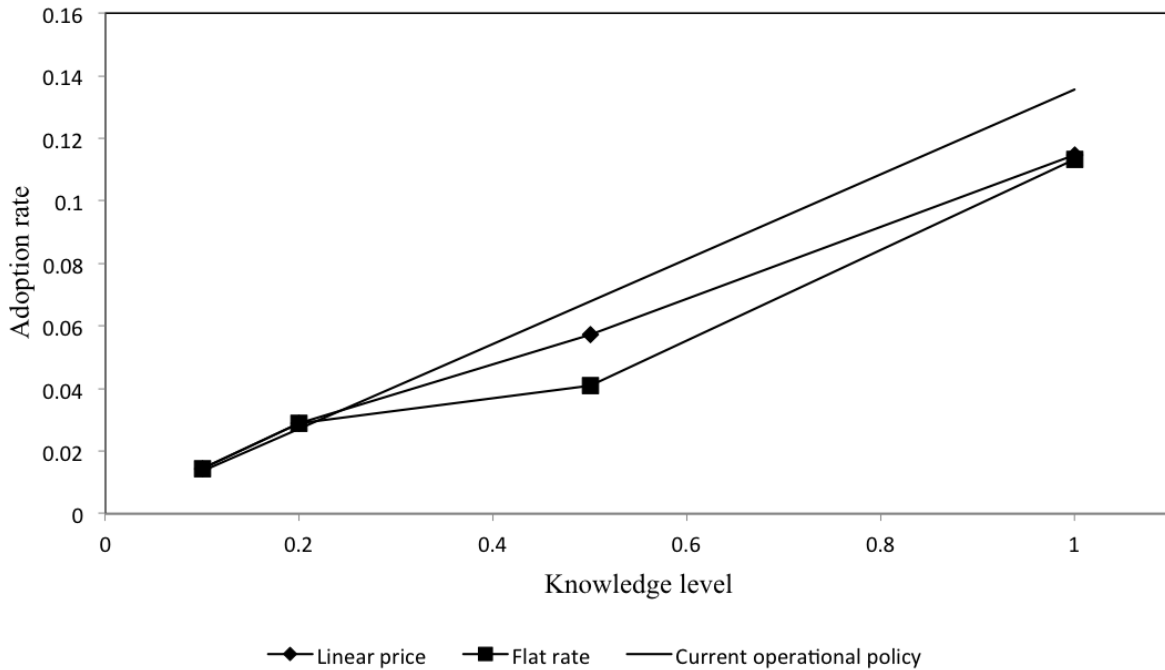
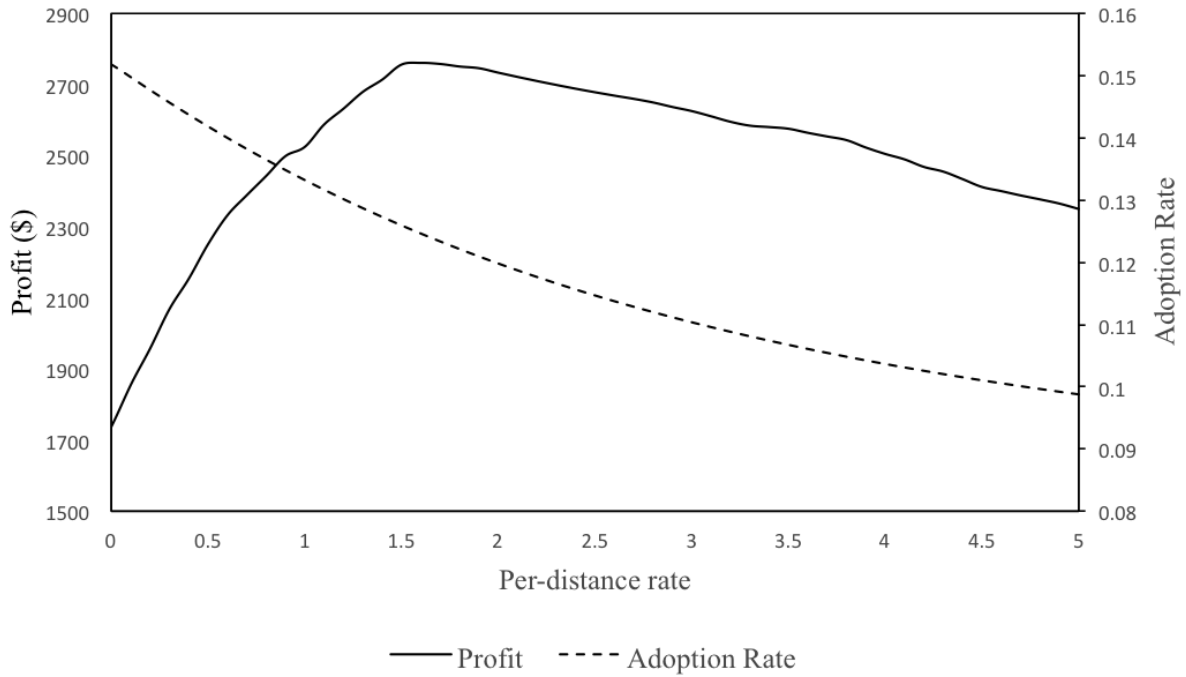


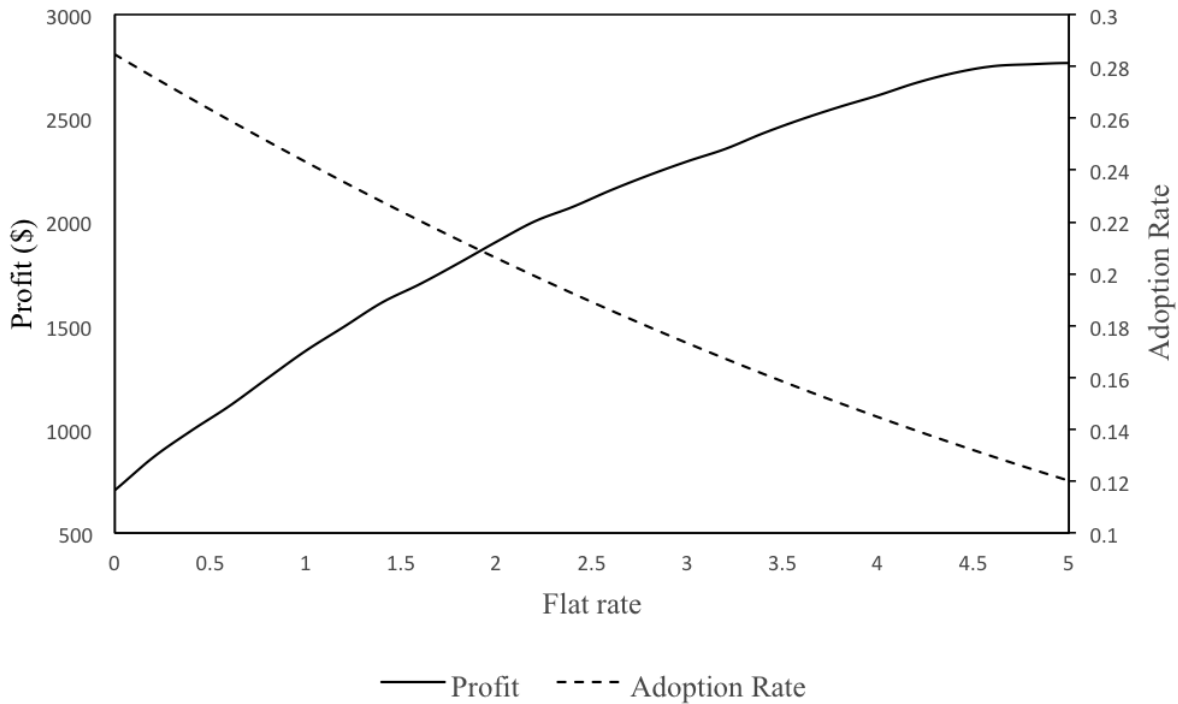
Figure 2.8: Comparing adoption rates

Figure 2.7 illustrates the comparison between optimal profits in the three cases considered under different knowledge rates. As expected, in each case, the profit increases with knowledge rate. The current operational policy can not profit unless the knowledge rate is higher than around 0.5. Both case (ii) and (iii) significantly improve profitability of the service compared to the current operational policy, suggesting that the current operational policy provides excessive capacity. The improvement in profit from including distance based price is relatively moderate, varying from less than 1% to 8.9%. This perhaps surprising result is a result of existing competition, that is, the competing modes' pricing policy are predominantly flat-rate only. As a result, the benefit of charging a per-distance price is limited by the reduced competitive advantage. This is further reflected in the phenomenon that the optimal per-distance rate is increasing in the knowledge level as increased knowledge level enhances RS's competitiveness. These results highlights the

advantage of incorporating competing mode choices in the demand model compared to traditional demand function forms.



(a). Varying per-distance price c_1 (fixing c_2 at \$4.7659)



(b). Varying flat rate c_2 (fixing c_1 at \$1.5268/mi)

Figure 2.9: Trade-off between profit and adoption rate (at knowledge level 1)

Figure 2.8 illustrates the comparison between adoption rates of RS in the three cases considered under different knowledge rates, where adoption rate of a travel mode is defined as the trips served by the mode divided by the total travel demand that can be served by this mode. Clearly, current policy obtains the highest adoption rate due to the excessive capacity the service provides. The adoption rates under linear pricing policy are higher than those under flat-rate only policy, especially for intermediate knowledge levels.

It is not difficult to see that there existing a tradeoff between profit and adoption rate. Figures 2.9a and 2.9b illustrate this tradeoff by varying the per-distance rate and flat rate, respectively. We can see that in reducing price from optimality, adoption rate is improved at the expense of profitability. However, interestingly, we observe that the profit decreases at a lower rate than the adoption rate increases in the neighborhood of the optimal price. This effect is

particularly strong when varying the flat rate. For example, reducing the flat rate from \$4.8 to \$4.6 leads to a 3.5% increase in adoption rate with only 0.4% decrease in profit. This effect suggests an opportunity to significantly increase adoption rate with little compromise on profit, which has important implications as customer adoption is critical to the success of a startup in a competitive environment.

In addition, we study the shift of adoption rates of travel modes before and after RS enters the market. In particular, we aim to answer the question “what modes are most affected by RS’s market entry in NYC?”. Table 2.9 summarizes the estimates of the market shares of the travel modes with and without RS. Comparing the results from Tables 2.9a and 2.9b suggests that RS mainly attracts customers who originally chose transit or walk modes for their commuting trips.

Table 2.9: Estimate adoption rate of travel modes

Mode	Adoption Rate
Auto	1.53%
Transit	37.12%
Via	14.37%
Walk	46.98%

(a). Without RS

Mode	Adoption Rate
Auto	1.34%
Transit	32.66%
Via	12.55%
Walk	40.89%

RS	12.56%
----	--------

(b). With RS

2.6 Conclusion

In this chapter, we investigated the pricing and operational policy design problem for a fixed-route ride-sharing service. To solve the challenge of estimating the demand of the service, we developed a choice model based on multinomial logit mode-choice model. Using publicly available travel survey data, we showed that this model is effective in predicting customer mode-choices and therefore demand of the service. Using this model, we then constructed an optimization model for the joint planning of price, fleet size and shuttle frequency.

In a case study of a real-world fixed-route ride-sharing service in NYC, we calculated the optimal prices and operational policies for varying levels of commuter knowledge of RS. Our results suggest that jointly optimizing price and operational policy significantly improves profitability of the service compared to optimizing only price under the current operational policy, and that the optimal departure interval is substantially larger than the current value. We also find that having a distance-based price only moderately affect the profitability of the service, and its effect on the adoption rate may be more notable. In addition, we illustrated the tradeoff between profit and adoption rate, and highlighted the opportunity for significantly increasing the adoption rate with little compromise of profit by reducing the flat rate from its optimal value. Moreover, our results suggest that RS's customers are predicted to be predominately diverted from those who either took transit or walk to commute in the absence of RS.

Chapter 3: Fixed Route Design

3.1 Introduction

One of the most commonly used ridesharing services is public transit, e.g., buses. It offers shared rides along fixed routes with predetermined stations, usually at a fixed fee and operating according to a prearranged timetable. In recent years, more and more privately owned fixed route ride-sharing companies, such as Chariot, Boxcar Transit, and OurBus, have entered the market. Ridesharing services are generally regarded as having higher energy efficiency than other comparable modes of travel through combining common trip segments among passengers. Fixed-route ridesharing services may either be profit driven or funded by governmental subsidies. No matter the type of service, a key objective of these services is to increase their ridership. This has multiple benefits: first, it allows these services to increase their revenue; second, it permit high utilization of their capacity and therefore enhance their energy efficiency; third, increasing ridership of the service allows it to serve more travel needs; fourth, more travel demand served through ridesharing reduces single-occupancy vehicles and thus reduce congestion. In this chapter, we investigate the design of a ridesharing system in order to maximize ridership/demand of the service. Specifically, we determine the number of routes within the service area, stations on each route and the order of visiting each station.

Transit network design (TND) is one of the most crucial decision to the sustainable urban development (Ibarra-Rojas et al. (2015)). A well-designed transit network can impact the travel

time, road congestion, city pollution and road accident. As rapid development of urban area worldwide, TND is attracting increasing research interests. TND specifies designs including line layout, stop spacing and vehicle headways to meet the requirement of the objective function. Researchers have investigated the optimal design for achieving different objectives, e.g., minimizing cost, minimizing the number of transfers, maximizing social welfare and maximizing direct trips etc. The problem in the chapter can be viewed as a TND problem. However, different from the TND literature where demand is predominantly assumed to be fixed and continuous, we treat the travel demand as discrete and dependent with the configuration of the routes. For example, adding a new station on a route will affect the demands between all existing stations and with the new station. As a result, the model developed in this chapter contribute to not only the line layout design but also the vehicle headway design.

The design of a fixed-route ride-sharing service is similar to the vehicle routing problem with pickup and delivery (VRPPD). In the VRPPD, a number of routes have to be constructed in order to satisfy a set of transportation requests, each of which specifies its origin and destination. One or more capacitated vehicles depart from and arrive at a central depot, and operate round trips between customers' locations and depot. The objective of the VRPPD usually is to minimize the total cost for satisfying all transportation requests. The solution of the VRPPD determines the assignment of vehicles to customers, as well as each vehicle's order of visiting its assigned customers. Similar to the VRPPD, the routing design problem we consider for the ride-sharing service also determines grouping of stations and the order of visiting each station, given a set of potential stations and potential travel requests. However, the ridesharing routing design problem in this paper differs from the traditional VRPPD in the following sense. First, in the conventional VRPPD, all customer nodes are visited exactly once. However, in the ridesharing routing design

problem considered in this chapter, a station node can be visited by multiple routes or never visited by any route. Second, the objective of the VRPPD is to minimize the total cost of operation, whereas the objective of the ridesharing routing design problem is to maximize the total demand served. Third, a crucial difference is that the demand of each node in the ridesharing routing design problem depends on other nodes on the route. For example, if a new station is added to an existing route, then the total demand on this route is increased by the demand covered between the new station and all the existing stations on the route. In contrast, the demand is fixed independent of the route configuration in the VRPPD. Lastly, the VRPPD considers the capacity of the vehicles while the shuttle's capacity is not considered as a constraint in the ride-sharing routing design problem. This is because when the capacity of each route can be easily adjusted by changing the shuttle departure frequency.

In this chapter, we formulate the ridesharing routing design problem as a mixed integer linear programming (MILP) optimization problem. Because the problem is NP-hard, we then propose a heuristic based on Genetic Algorithm (GA) for improving the solution efficiency. Using a number of test instances, we find that the proposed algorithm leads to solutions that have close performance compared to the MILP optimal solutions (with objective values of less than 10% higher than the MILP optimal objective value). We also apply the model and algorithm in a case study with a large number of potential stations (288 in total), in which we find the optimal routes in Manhattan to maximize ridership of the service.

The rest of this chapter is organized as follows. Section 2 offers a review of related literature. Section 3 describes the model setup and formulates the ridesharing routing design problem as a MILP. Section 4 proposes a GA based heuristic approach to solve the problem. Section 5 provides a case study based on real-world data from New York City (NYC), in which

optimal routes are selected to satisfy the demand of NYC commuters. Finally, Section 6 offers concluding remarks.

3.2 Literature Review

The fixed-route ride-sharing routing design problem presented in this chapter is closely related to the vehicle routing problem with pickup and delivery (VRPPD). Dantzig et al. (1954) introduce the vehicle routing problem as an extension of the traveling salesman problem and proposed several solutions to the problem. Dantzig & Ramser (1959) construct a capacitated vehicle routing problem to find the optimal route to deliver goods to various customers. In this problem, each customer has a demand for goods and vehicle have a limited capacity. A number of papers studied the VRP extension with time window constraints (VRPTW), e.g., Golden & Assad (1986), Assad (1988) and Lenstra et al. (1988). The pickup and delivery problem with time windows (PDPTW) (Cordeau et al. (1997), Ropke & Pisinger (2006)) is considered as the generalization of VRPTW. In this problem, customers' request is associated with 2 locations: an origin where customer should be picked up and a destination where customer should be dropped off. For each route, the origin must precede the destination and both locations are on the same route. However, the classic PDPTW differ from the ridesharing routing design problem investigated in this chapter in that the total demand served by the routes in this chapter depends on the routing design. In addition, the objective of our problem is to maximize the total demand served by the routes, which also differs from the PDPTW literature which typically focuses on minimizing the total cost or minimizing the total travel time.

The design of fixed-route ride-sharing systems is also discussed the transit network design (TND). TND determines the number and locations of transit stops, the headway, and the general

line layout in a predefined service region. Generally, the service zone for a public transit can be described based on a network $N(V, A)$. V represent a set of geographic stops that can be connected by arcs $(i, j) \in A$, where A is a set of arcs and $i, j \in V$. Decisions for TND include the transit stops location, the visit sequence for the stops and the average spaces between two stops. There're multiple objectives for TND such as minimize the total users' and operator's cost, minimize the number of transfers, minimize the number of unsatisfied passengers, maximize the direct trips etc. As a result, many researchers combine multiple objectives as the final objective function. The TND problem is traditionally solved using one of two approaches: continuous approximation and discrete optimization. The continuous approximation approach analytically models the passengers' demands as a continuous function over a geographic space. For example, Chien & Spasovic (2002) consider an elastic demand dependent on the level of service of the transit with the objective of maximizing the social welfare, i.e., sum of customer surplus and operator's profit. Daganzo (2010) assumes uniform demand in a square service region and solves for the transit network structure that minimizes the total cost. However, the relationship between demand and geographic factors is dynamic and unpredictable, and the performances of demand models are also difficult to validate. As a result, most authors have modeled the TND problem as discrete optimization problems. For example, Fan & Machemehl (2006b) assume fixed demand and minimize the weighted sum of operator cost, user cost, and unsatisfied demand cost. Nayeem et al. (2014) solve the TND with static demand to minimize the weighted sum of total number of unsatisfied passengers, the total number of transfers and the total travel time of all served passengers. Nikolic' and Teodorovic' (2013) also solve the static demand by minimizing the number of transfers and the total travel time. In this chapter, we also model the fixed-route ride-sharing design problem as a discrete

optimization. However, differing from the TND literature, the objective our model is to maximize the total demand served by the routes while the demand is endogenous to the routing design.

Solving the TND discrete optimization problem is challenging as the problem is often NP-hard (Lenstra & Kan 1981). Several papers have applied exact algorithms such as the branch-and-cut algorithm (Carpaneto et al. 1989) or the column generation algorithm (Desrochers et al. 1992) to solving the problem. However, exact algorithms are only tractable for restricted size problems, e.g., small instances (Wan and Lo 2003) or design of a single line (Guan et al. 2003). As a result, meta-heuristic methods have been introduced. Existing meta-heuristic approaches for the TND problem include: Tabu Search (Fan & Machemehl 2008), Simulated Annealing (Fan & Machemehl 2006b) and population-based algorithms like genetic algorithm (Fan & Machemehl 2006a) and artificial bee colony algorithm (Szeto & Jiang 2012). Among these methods, the genetic algorithm (GA) has gained increasing popularity as it can be naturally embedded into the TND problem (Chakroborty 2003), where line generation can be iteratively obtained through a similar process to chromosome crossover and mutation. Some recent examples of applying GA to solving TND problems include Fan & Machemehl (2006a), Chakroborty (2003) and Amiripour et al. (2014). The use of GA has been proven to significantly shorten the computational time compared to other heuristics while generating relatively good approximations to the exact optimal solutions. In this chapter, we also propose a GA based approach for solving the ride-sharing routing design problem, with more details described in Chapter 3.

3.3 Model Formulation

We consider a set of potential stations Φ . A pseudo origin β and a pseudo destination $\bar{\beta}$ are introduced in addition to the set of stations to represent the start or the end of all routes, respectively.

We denote the set of potential stations including origin β as Φ_β , and denote the set of potential stations including destination $\bar{\beta}$ as $\Phi_{\bar{\beta}}$. Let \mathcal{R} denotes the set of routes to be generated for the service. p_{ij} denotes the total potential demand with origin in the service region of station i and destination in the service region of station j . d_{ij} represents the direct travel distance between station i and station j . L is the maximum allowed route length, and WD is the minimum distance between two adjacent stations on any route. x_{ija} is a binary decision variable, with $x_{ija} = 1$ indicating that station i is immediately followed by station j on route a , and $x_{ija} = 0$ otherwise. y_{ia} is another binary decision variable, with $y_{ia} = 1$ indicating that station i is visited by route a , and $y_{ia} = 0$ otherwise. s_{ija} and z_{ij} are variables that represent the sequences of stations. $s_{ija} = 1$ indicates that station i is visited before station j on route a , and $s_{ija} = 0$ otherwise. z_{ij} is a similar variable with $z_{ij} = 1$ indicating that station i is visited before station j on at least one of the routes, and $z_{ij} = 0$ otherwise. D_{ja} defines the position of station j on route a , i.e., D_{ja} is the distance of travel between route a 's origin and station j following route a . Table 3.1 summarizes the parameter definitions in the model.

Table 3.1: Parameters Definition

Parameter	Definition
Φ	A set of potential stations.
β	A pseudo origin.
$\bar{\beta}$	A pseudo destination.
Φ_β	A set of potential stations including pseudo origin β .
$\Phi_{\bar{\beta}}$	A set of potential stations including pseudo destination $\bar{\beta}$.

- p_{ij} Total potential demand from station i to station j , $i, j \in \Phi$.
- d_{ij} Direct travel distance between station i and station j , $i, j \in \Phi$.
- L Maximum length of a route.
- WD Minimum distance between two adjacent stations on a route.
- M A large number.
- x_{ija} Binary decision variable that indicates whether station i immediately before station j on route a .
- y_{ia} Binary decision variable that indicates whether route a serves station i .
- s_{ija} Binary decision variable that indicates whether station i is visited before station j on route a .
- z_{ij} Binary decision variable that indicates whether station i is visited before station j on at least one route.
- D_{ja} Travel distance between station j and station β on route a , $D_{\beta a} = 0$.
- w_{ija} A variable introduced to linearize the model, $w_{ija} = D_{ia} \times x_{ija}$.
-

We build the mixed integer programming (MIP) model to solve the routing design problem for the fixed-route ride-sharing service as follows:

$$\text{Maximize } \sum_{i,j \in \Phi} p_{ij} z_{ij}, \quad (3.1)$$

$$\text{s. t. } \sum_{i,j \in \Phi} d_{ij} x_{ija} \leq L, \quad \forall a \in \mathcal{R} \quad (3.2)$$

$$d_{ij} \geq 2 \times WD \times x_{ija}, \quad \forall i, j \in \Phi, a \in \mathcal{R} \quad (3.3)$$

$$y_{\beta a} = 1, y_{\bar{\beta} a} = 1, \quad \forall a \in \mathcal{R} \quad (3.4)$$

$$\sum_{i \neq j, i \in \Phi_{\beta}} x_{ija} = y_{ja}, \quad \forall j \in \Phi_{\bar{\beta}}, a \in \mathcal{R} \quad (3.5)$$

$$\sum_{i \neq j, j \in \Phi_{\bar{\beta}}} x_{ija} = y_{ia}, \quad \forall i \in \Phi_{\beta}, a \in \mathcal{R} \quad (3.6)$$

$$\sum_{j \in \Phi} x_{\bar{\beta}ja} = 0, \quad \forall a \in \mathcal{R} \quad (3.7)$$

$$\sum_{i \in \Phi} x_{i\beta a} = 0, \quad \forall a \in \mathcal{R} \quad (3.8)$$

$$D_{ja} = \sum_{i \in \Phi_{\beta}} (D_{ia} + d_{ij} \times x_{ija}), \quad \forall j \in \Phi_{\bar{\beta}}, a \in \mathcal{R} \quad (3.9)$$

$$D_{ia} + d_{ij} \leq D_{ja} + M \times (1 - s_{ija}), \quad \forall i, j \neq i \in \Phi, a \in \mathcal{R} \quad (3.10)$$

$$z_{ij} \leq \sum_{a \in \mathcal{R}} s_{ija}, \quad \forall i, j \in \Phi, a \in \mathcal{R} \quad (3.11)$$

$$x_{ija}, y_{ia}, s_{ija}, z_{ij} \in \{0,1\} \quad \forall i, j \in \Phi, a \in \mathcal{R} \quad (3.12)$$

The objective of the MIP is to maximize the total direct travel served by the routes. Constraint (3.2) imposes the maximum route length limit. Constraint (3.3) specifies the minimum distance restriction between adjacent stations on any route. Constraint (3.4) ensures that every route starts from β or ends at $\bar{\beta}$. Constraints (3.5)-(3.6) guarantees that there are no circles in the routes, i.e., each station is visited once and only once on a route. Constraints (3.7)-(3.8) specifies that β does not have any upstream stations, and $\bar{\beta}$ does not have any downstream stations. Constraint (3.9) follows the definition of D_{ia} and make sure that the value of D_{ia} is consistent with the value of x_{ija} . That is, if station i is visited before station j on route a , D_{ja} should be greater than D_{ia} . Constraint (3.10) ensures that the values of D_{ja} and s_{ija} are consistent. That is, the

distance of a station i is farther from the origin on route a than station j if and only if station i is visited before station j on route a . Constraint (3.11) guarantees consistency between s_{ija} and z_{ij} , that is, if station i is not visited before station j on any route a then $z_{ij} = 0$. Finally, (3.12) specifies binary constraints.

Constraint (3.9) is not a linear constraint. To linearize the model, we introduce an additional decision variable $w_{ija} = D_{ia}x_{ija}$ and a sufficient large number M . Model (3.1)-(3.12) can thus be linearized as follows:

$$\text{Maximize } \sum_{i,j \in \Phi} p_{ij} z_{ij}, \quad (3.1)$$

$$s. t. \quad D_{ja} = \sum_{i \in \Phi_\beta} (w_{ija} + d_{ij} \times x_{ija}), \quad \forall j \in \Phi_\beta, a \in \mathcal{R} \quad (3.13)$$

$$w_{ija} \leq D_{ia}, \quad \forall i, j \in \Phi, a \in \mathcal{R} \quad (3.14)$$

$$w_{ija} \leq M \times x_{ija}, \quad \forall i, j \in \Phi, a \in \mathcal{R} \quad (3.15)$$

$$w_{ija} \geq D_{ia} - (1 - x_{ija}) \times M, \quad \forall i, j \in \Phi, a \in \mathcal{R} \quad (3.16)$$

$$w_{ija} \geq 0, \quad \forall i, j \in \Phi, a \in \mathcal{R} \quad (3.17)$$

$$(3.2)-(3.8), (3.10)-(3.12)$$

The above MILP model is similar to the VRPPD with no capacity constraints, and can be proven to be NP-hard (Lenstra, J. K., & Kan, A. R. (1981)) as the problem can be stated as a spanning tree which is exponentially grow with the number of iterations. As a result, a heuristic algorithm is needed to solve the problem within reasonable time. In the next section, we propose a genetic algorithm based approach for solving the MILP.

3.4 Genetic Algorithm Based Approach

In this section, a GA-based approach is developed to solve the routing design problem presented in Section 3.4. The basic steps of genetic algorithm are: first, initializing the population; second, decoding chromosome; third, selecting individuals from the population for breeding the new generation; fourth, breed the new generation through GA operators (crossover and mutation); finally, survivals are realized based on fitness evaluation (Tasan & Gen 2012). These steps are illustrated in Figure 3.1.

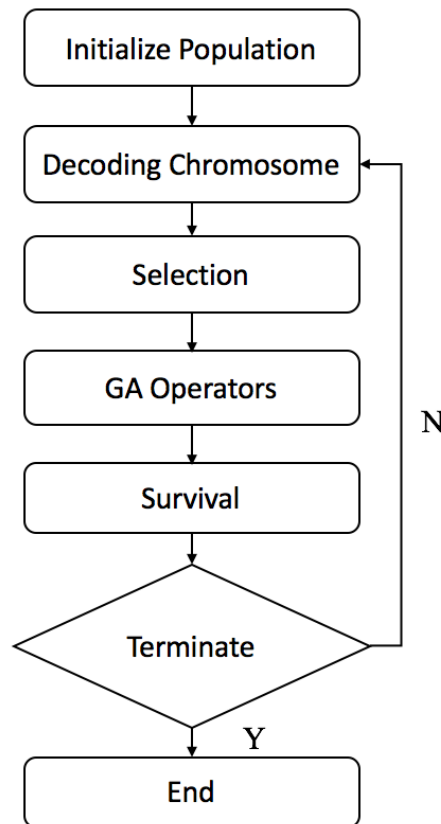


Figure 3.1: General Procedure of Genetic Algorithm
(figure adapted from Tasan, & Gen 2012)

Table 3.2: Procedure for the Proposed GA Approach

Procedure:	GA for Ride-sharing Routing Design
Input:	location data for potential stations, commuter traveling demand, GA parameters
Output:	The optimal routes (routes with the largest total demand served)
Initialize:	$t \leftarrow 0$; Initialize $P(t)$ by using random permutation; Evaluate $P(t)$ by calculating the fitness value;
While	the stopping criterion not satisfied do
	For each iteration i
	Parents $P_{i1}(t), P_{i2}(t)$ are selected from $P(t)$
	$P_{i1}(t)$ and $P_{i2}(t)$ crossover to produce offspring O_{i1}
	Offspring O_{i1} mutate with a probability to generate offspring O_{i2}
	O_{i1}, O_{i2} constitute child $C_i(t)$
	End
	All $C_i(t)$ compose child generation $C(t)$
	Evaluate the fitness value of $C(t)$ and $P(t)$, respectively
	Select the next generation $P(t + 1)$ from $P(t)$ and $C(t)$
	$t + 1 \leftarrow t$
	End
Output	the best routes
End	

Table 3.2 presents the procedures of the proposed GA algorithm. Parameter t denotes the number of generations. $P(t)$ refers to the whole population at generation t . In our problem, $P(t)$

corresponds to a set of different routing solutions. $P_{i1}(t)$ and $P_{i2}(t)$ denote 2 parents selected from the whole population $P(t)$ in iteration i . Through crossover and mutation operations, the parents produce the next generation $C(t)$. We detail the steps in the procedure below.

3.4.1 Genetic Representation and Encoding

The genes in this problem represent the potential stations with unique geo-locations, which we can illustrate using the permutation representation for the genetic representation; see Figure 3.2. In biology, genes constitute a chromosome and chromosomes define an individual. Analogously, in our problem, various stations in different orders constitute a route and a collection of routes form a preliminary solution. Therefore, a potential station can be considered a “gene” in the GA, a route corresponds to a “chromosome”, a solution becomes an “individual”, and the set of solutions is a “population”.

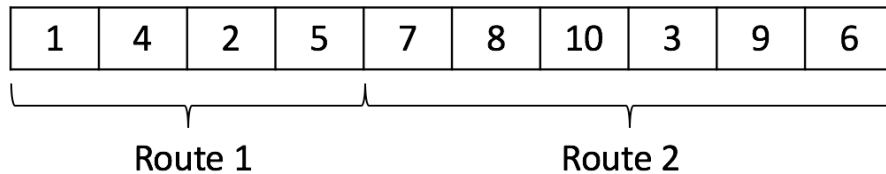


Figure 3.2: Genetic representation of the routing design problem

3.4.2 Initialization

The population size is a GA parameter that is predefined. Moreover, the initial population should be generated in advance to further produce the offspring. We use random permutation to construct the initial population. Specifically, the stations are randomly chosen and assigned to a route as long as the route length and station distance constraints are not violated.

3.4.3 Fitness value

The fitness value of an individual determined by the fitness function (3.19) directly determines the probability that an individual is selected for survival. The individuals with higher fitness values are more likely to survive while those with lower fitness values have a higher probability to be removed from the population. Therefore, a feasible solution should have a higher fitness value than an infeasible solution. To avoid infeasible routes, high penalties are added to the fitness function for when the route length exceeds the length constraint and/or the distance between stations is less than the minimum allowable station distance.

$$\text{Fitness Value} = \sum_{i,j \in \Phi} p_{ij} z_{ij} - \text{Penalty}(\text{Route Length}) - \text{Penalty}(\text{Station Distance}) \quad (3.19)$$

3.4.4 Selection

The idea behind selection is to identify the fittest individuals and let them pass their genes to the next generation. The roulette wheel selection method is used in the approach in this chapter. To make sure that the sum of fitness values of all individuals is 1, we scale all the values to be within (0,1). The probability of being selected for an individual is directly proportional to its fitness value. For instance, in Figure 3.3, the individual P1 has the highest fitness value ($F1 = 0.34$), so the probability for P1 to be selected is also the highest.

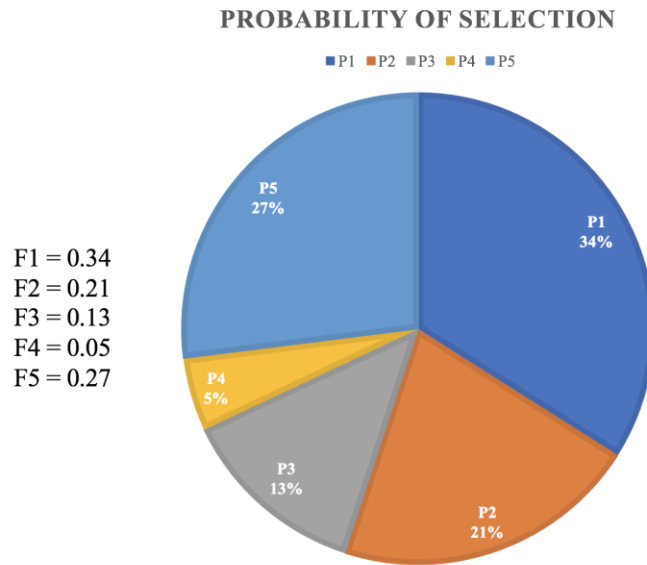


Figure 3.3: Roulette Wheel Selection

3.4.5 Crossover

Crossover is a genetic operator that simulates the reproduction of the next generation between two parents. It works on a pair of solutions by recombining them in a certain way to generate offspring. The offspring shares some similar characteristics with its parents, and does not create any new characteristics that are different from those of the parents. The probability of crossover is a predetermined GA parameter. We use simple random crossover in this chapter. The procedure for this method is shown in Table 3.3.

Table 3.3: Simple random crossover procedure

Procedure	Simple Random Crossover (SRC)
Input	Two Parents (P_1, P_2), crossover probability p_c
Begins:	Do while $p_c \geq rand()$

Copy individual P_1 into offspring O_1

Randomly select a sub-route s_1 from P_2

Delete the corresponding genes in s_1 from the offspring O_1

Randomly select a position on O_1

Insert the s_1 at the selected position to generate new O_1

End

Output Offspring O_1

End

3.4.6 Mutation

Different from the crossover operator, the mutation operator is applied to a single solution and it can generate new characteristics that are distinct from those of its parents. The mutation operator makes small random changes in the solution with a relatively low probability. We use the simple random mutation method (SRM) to simulate the process of mutation. The detailed procedure of SRM is described in Table 3.4.

Table 3.4: Simple random mutation procedure

Procedure Simple Random Mutation (SRM)

Input A single Parent P_1 , mutation probability p_m

Begins: **If** $p_m \geq rand()$

 Randomly select a route r_1 from P_1

 Randomly select a station s_1 from P_1

	If $s_1 \in r_1$
	Delete the station s_1 from the route r_1
	Else
	Randomly select a position to insert the s_1 using best insertion method ¹
	Insert s_1 into r_1 at the selected position
	End
Output	Offspring
End	

3.5 Case Study

In this section, we discuss the application of the proposed model and algorithm using a case study. First, a brief overview of the case study problem is provided. Second, parameters estimates in the case study are discussed. Third, the solution and performance of the proposed GA algorithm under different parameters are presented. Finally, a comparison between the performance of the proposed GA based approach and the exact algorithm is conducted for validation purpose.

3.5.1 Problem Statement

This case study is based on Manhattan, NYC. We assume that the center of each census tract is a potential station to be served. This treatment is selected as the sizes of census tracts are sufficiently small (consisting of roughly 39 blocks). There are total of 288 census tracts in Manhattan area. Therefore, we have 288 potential stations as shown in Figure 2.2a. The objective

¹ Best insertion method: The sub-route is inserted into the route with the biggest improve to the objective value.

of this case study is to select 3 routes that directly serve the most commuter travel demand in Manhattan. The proposed GA based approach described in section 3.2 is used to solve the case problem. Different combinations of GA parameters are tested to find the optimal routes in the next section. The solution provides new route suggestions for a fixed route ride-sharing service operating in Manhattan.

3.5.2 Parameter Estimation

In this section, we provide estimates for the input parameters of the model. The distance between station i and station j , d_{ij} , is estimated as the Manhattan distance between the geo-locations of stations i and j . A sample of the estimates is shown in Figure 3.4 below. The potential travel demand between station i and station j , p_{ij} , is estimated as the commuter travel demand provided in the CTPP 2006-2010 Census Tract Flows (CTF) data. Figure 3.5 shows a sample of potential demand within Manhattan.

0	0.29662343	0.54727349	0.79436979	0.88466683	1.06614675	0.86903743	0.7716314	0.71852452	2.16554253	2.33932536	2.72618926	2.78099133	2.79050128	2.85625135	2.63315655	2.70799625	2.93477104
0.29662343	0	0.25050502	0.49774638	0.63229988	0.86820244	0.74090563	0.71307172	0.7395932	2.2065321	2.40137923	2.80878064	2.88146264	2.91951207	3.00649988	2.8004669	2.89007209	3.10303791
0.54727349	0.25050502	0	0.24709646	0.46234895	0.75360631	0.71576918	0.75676934	0.84300266	2.27133782	2.48074116	2.9008029	2.98708718	3.04714405	3.1499858	2.95797761	3.05820288	3.25980651
0.79436979	0.49774638	0.24709646	0	0.39108049	0.7119975	0.77360402	0.87077696	0.99710808	2.35918477	2.58003399	3.00878598	3.10707805	3.18686277	3.30356917	3.12480467	3.23406325	3.42491578
0.88466683	0.63229988	0.46234895	0.39108049	0	0.32091744	0.43896216	0.59377387	0.7675111	2.00689128	2.23567767	2.6697298	2.77914281	2.88062519	3.01476783	2.85690359	2.9803632	3.15231973
1.06614675	0.86820244	0.75360631	0.7119975	0.32091744	0	0.29770343	0.49886593	0.69720393	1.73068358	1.96661232	2.40375674	2.52396893	2.64659029	2.79695822	2.66054187	2.79654645	2.94918659
0.86903743	0.74090563	0.71576918	0.77360402	0.43896216	0.29770343	0	0.20116674	0.39950874	1.58576057	1.80859261	2.23980651	2.34454822	2.44190673	2.57620979	2.42178341	2.54887651	2.71590601
0.7716314	0.71307172	0.7395932	0.87077696	0.59377387	0.49886593	0.20116674	0	0.19834241	1.51496016	1.72442927	2.14690529	2.2391021	2.31640045	2.43758682	2.26948867	2.38905112	2.56699409
0.71852452	0.7395932	0.84300266	0.99710808	0.7675111	0.69720393	0.39950874	0.19834241	0	1.46953792	1.66178905	2.07095262	2.14906845	2.20415288	2.31038247	2.12770709	2.23838916	2.42797817
2.16554253	2.2065321	2.27133782	2.35918477	2.00689128	1.73068358	1.58576057	1.51496016	1.46953792	0	0.24709036	0.68092972	0.82562371	1.02411886	1.23754543	1.23292997	1.41680656	1.44699314
2.33932536	2.40137923	2.48074116	2.58003399	2.23567767	1.96661232	1.80859261	1.72442927	1.66178905	0.24709036	0	0.43777123	0.5785935	0.7879148	1.0111866	1.03912729	1.22690336	1.22845791
2.72618926	2.80878064	2.9008029	3.00878598	2.6697298	2.40375674	2.23980651	2.14690529	2.07095262	0.68092972	0.43777123	0	0.18850466	0.47909749	0.72598118	0.86715241	1.04797522	0.95738047
2.78099133	2.88146264	2.98708718	3.10707805	2.77914281	2.52396893	2.34454822	2.2391021	2.14906845	0.82562371	0.5785935	0.18850466	0	0.29760347	0.54313422	0.71089481	0.88435982	0.77408468
2.79050128	2.91951207	3.04714405	3.18686277	2.88062519	2.64659029	2.44190673	2.31640045	2.20415288	1.02411886	0.7879148	0.47909749	0.29760347	0	0.24688752	0.43776391	0.59759876	0.47828639
2.85625135	3.00649988	3.1499858	3.30356917	3.01476783	2.79695822	2.57620979	2.43758682	2.31038247	1.23754543	1.0111866	0.72598118	0.54313422	0.24688752	0	0.28818048	0.39415625	0.23139947
2.63315655	2.8004669	2.95797761	3.12480467	2.85690359	2.66054187	2.42178341	2.26948867	2.12770709	1.23292997	1.03912729	0.86715241	0.71089481	0.43776391	0.28818048	0	0.18870185	0.30257598
2.70799625	2.89007209	3.05820288	3.23406325	2.9803632	2.79654645	2.54887651	2.38905112	2.23838916	1.41680656	1.22690336	1.04797522	0.88435982	0.59759876	0.39415625	0.18870185	0	0.27664484
2.93477104	3.10303791	3.25980651	3.42491578	3.15231973	2.94918659	2.71590601	2.56699409	2.42797817	1.44699314	1.22845791	0.95738047	0.77408468	0.47828639	0.23139947	0.30257598	0.27664484	0

Figure 3.4: Station distance

0	36061009800	3.6061E+10	3.6061E+10	3.6061E+10	3.6061E+10	3.6061E+10	3.6061E+10	3.6061E+10	3.6061E+10	3.6061E+10	3.6061E+10	3.6061E+10	3.6061E+10	3.6061E+10	3.6061E+10	3.6061E+10
36061009800	550	110	90	70	65	30	15	28	29	75	25	23	26	25		
36061010000	18	150	35	30	15	4	18	17	17	16	15	14	15	15		
36061010200	9	10	40	4	11	10	9	8	9	8	7	7	8	7		
36061010400	14	15	18	85	4	10	15	14	15	14	12	11	13	12		
36061011300	7	8	8	8	0	7	7	7	7	7	6	6	6	6		
36061011402	30	50	50	25	23	155	21	19	20	18	16	15	17	17		
36061013000	15	25	130	95	25	25	540	15	23	21	19	18	20	19		
36061014000	20	140	115	85	32	15	10	455	32	4	26	23	26	25		
36061014801	15	20	25	20	25	10	22	22	65	19	19	17	19	18		
36061015300	28	220	75	160	100	31	32	29	31	805	15	24	27	26		
36061015400	55	125	120	180	90	10	10	20	38	32	495	29	32	31		
36061018400	23	24	15	25	25	30	26	24	26	23	22	130	26	24		
36061019000	17	15	25	20	21	10	20	18	20	18	17	18	65	19		
36061020102	19	10	22	40	60	21	22	20	22	20	18	19	21	240		

Figure 3.5: Potential demand in Manhattan

The probabilities of crossover and mutation are also defined in advance for the GA based approach. As state in Section 3.4, p_c is much higher than p_m . Therefore, p_c is set as 0.9 and p_m is set as 0.02.

3.5.3 Result

To determine the appropriate population size and the number of generations for the GA, an initial test on different parameter combinations is conducted, including 9 combinations of population size and number of generations. For each combination, we run the GA 10 times and record the solutions after running each run using MATLAB 2017b. In Table 3.5, the best solution (column I, the best objective value obtained within the specified number of generations among the 10 runs), average of the GA solutions (column II, average objective value over number of generations over the 10 runs), worst of the GA solutions (column III, the worst value obtained within number of generations over 10 runs) and the average computation time in seconds (column IV, the CPU time) are provided.

Table 3.5: Computational results for parameter settings

Population Size	Number of Generations	I	II	III	IV
500	500	5738	5302	1245	353.69
500	1000	6248	5604.3	1478	938.24

500	1500	6357	5569.5	1406	1821.3
1000	500	7522	6111.4	1394	1411.5
1000	1000	8328	7121.8	1797	2058.5
1000	1500	7143	6542.5	1209	2169.6
1500	500	7460	6272.8	1432	1949.6
1500	1000	7502	6470.4	1643	2291.3
1500	1500	9818	8750.5	1851	4269.1
2000	2000	9905	8826.7	1546	6432.9

From Table 3.5, we can see that the objective value for combination (2000, 2000) is the highest. However, the objective values are only moderately improved from combination (1500, 1500), while the computational time is much higher than combination (1500, 1500). Therefore, we conclude that population size of 1500 and number of generation of 1500 is the most desirable. The best routes generated under this parameter setting are as follows:

Route 1: {171, 228, 252, 216, 217, 40, 61, 4, 101, 110}

Route 2: {37, 85, 32, 278, 166, 100, 58, 3, 136}

Route 3: {112, 107, 1, 75, 120, 286, 287, 284}

Figure 3.6 visualizes the resulting fixed routing design. The total demand served on the three routes is 9818, and the demands on each route are 3767, 3042 and 3009, respectively. Figure 3.7 illustrates the improvement of the objective value as the number of iterations increases. We can see that the objective value is always increasing in the number of iterations. The slope of the

plot is higher in first 500 iterations and become lower and lower after that. The routing design results of other parameter settings are provided in the appendix.

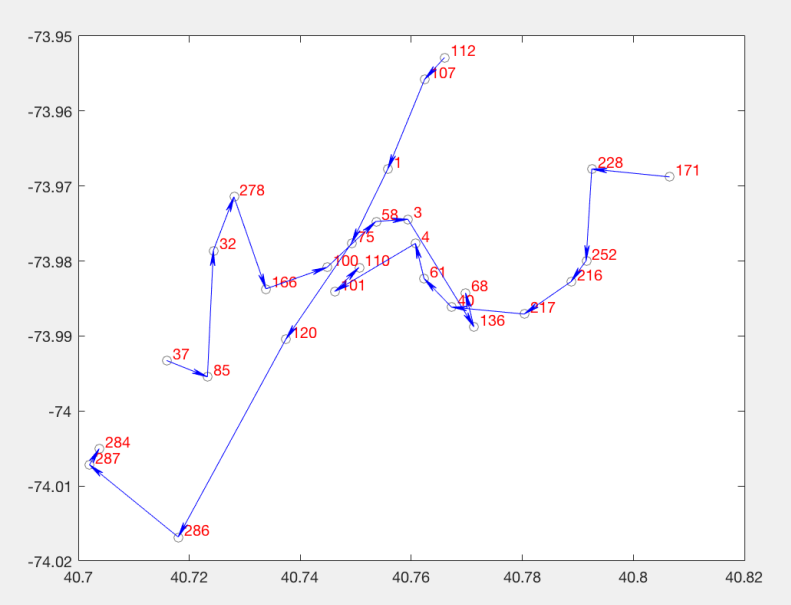


Figure 3.6: Best routing design generated by GA

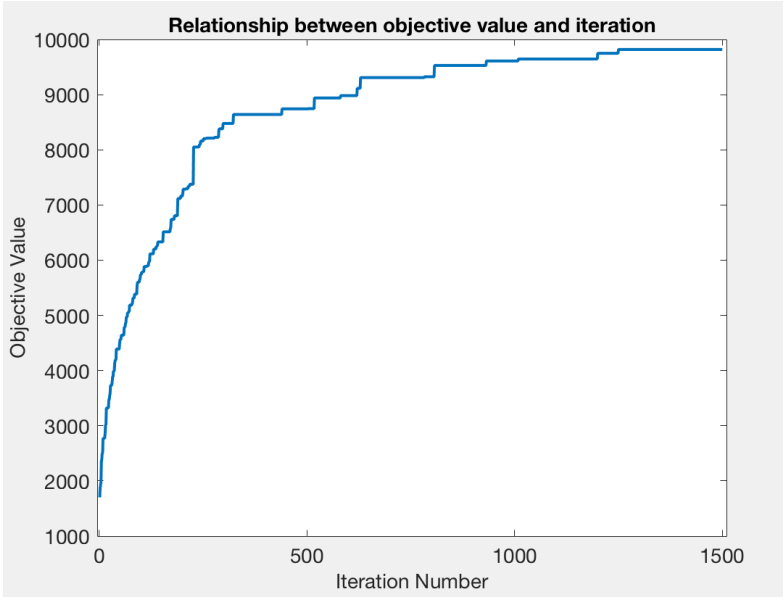


Figure 3.7: GA convergence plot

3.5.4 Validation

In this section, a validation is conducted to compare the results between the exact algorithm (MILP) and the proposed GA based algorithm. Due to the long computation time of the exact algorithm, the validation is performed on sample data of restricted sample sizes. We use MATLAB 2017b running the GA based algorithm and the MILP is solved in IBM CPLEX optimization studio.

Table 3.6: Results of validation on sample size of 20

Instances	GA-Best	MILP-Best	Differences
1	1934	2057	6.05%
2	2351	2547	8.34%
3	1904	2153	6.83%
4	1868	2023	8.30%
5	3678	3790	3.05%
6	2833	3055	7.84%
7	2693	2957	9.80%
8	1647	1758	6.74%
9	2112	2304	9.09%
10	1459	1540	5.55%

In the first set of validations, we compare the two approaches for problems with sample size 20 with the objective of selecting a single best route to maximize directly served travel demand. 10 problems are tested to cover most stations. Table 3.6 summarizes the validation results with objective values under the GA based algorithm (GA-Best) and the exact algorithm (MILP-Best). Figure 3.8 shows the scatterplot of GA-Best and MILP-Best. From the comparison results, we can find that the differences between GA-Best and MILP-Best are under 10% and 7.16% on average, indicating good performance for the proposed GA based method. Clearly, in such a small sized

problem, the computation time advantage of the GA based algorithm is not exhibited, while the exact algorithm can arrive at the optimal solution in a short time.

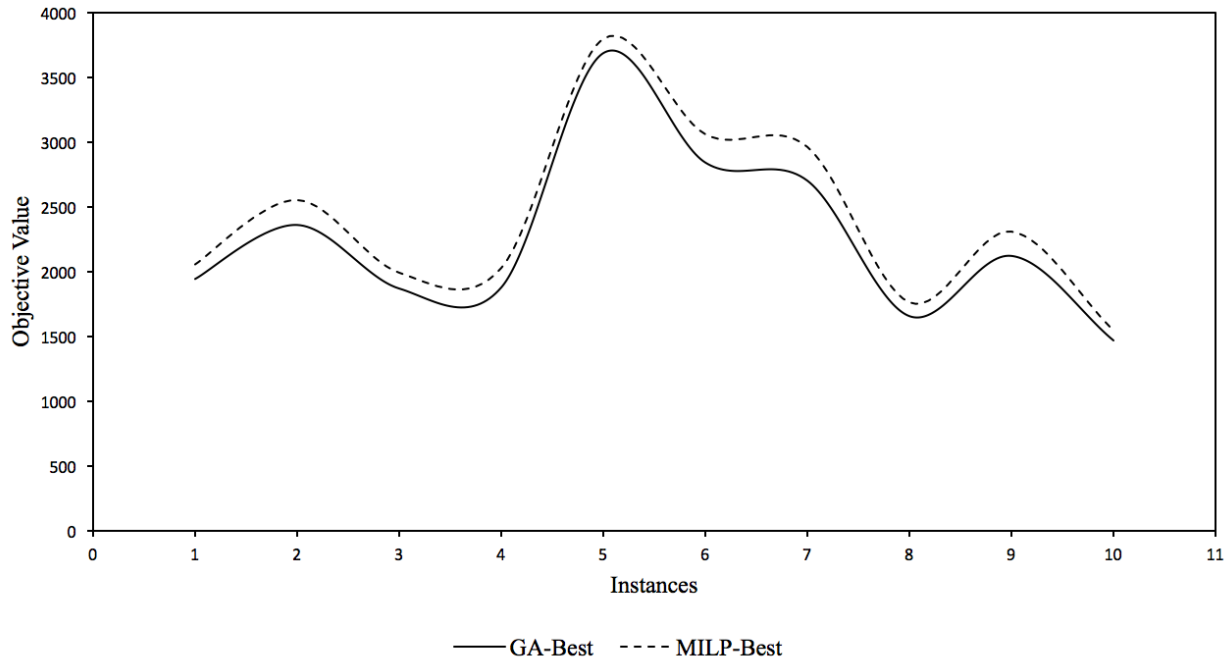


Figure 3.8: Comparison plot between GA and MILP on 20 sample size

In the second set of validations, we compare the two approaches for problems with sample size 30 and the objective of selecting the best two routes to maximize directly served travel demand. Due to long computation time of the exaction algorithm, we limit the computation time to 1 hour (3600 seconds) and supplement the results with the optimality gaps between the results obtained and the estimated optimal results. Table 3.7 summarizes the comparison results. We observe that the GA based algorithm objective values are only 4% higher than the exact algorithm on average, and may outperform the exact algorithm in some cases. The advantage of the GA over exact algorithm in terms of computation time also become evident in this set of results.

Table 3.7: Results of validation on sample size of 30 for 2 routes

Instances	MILP-Best	CPU Time	Optimality Gap	GA-Best	CPU Time	Differences
1	4620	3600	38.58%	4234	1232.52	9.12%
2	4547	3600	40.64%	4325	1124.67	5.23%
3	4980	3600	39.62%	4603	1197.54	8.19%
4	4128	3600	42.58%	4025	1256.95	2.56%
5	5745	3600	40.15%	5516	1203.68	4.15%
6	5439	3600	44.81%	5502	1297.49	-1.15%
7	4748	3600	42.17%	4423	1177.85	7.35%
8	4621	3600	38.96%	4410	1236.91	4.78%
9	6494	3600	41.38%	6285	1196.54	3.33%
10	4822	3600	43.89%	5007	1098.73	-3.69%

Comparing the results in Tables 3.6 and 3.7 we can see that as the problem size increases, the advantage of the GA based algorithm improves, in terms of both objective value and computation time. In general, we find the GA-based approach performs well in approximating the optimal solution of the fixed route ridesharing routing design problem.

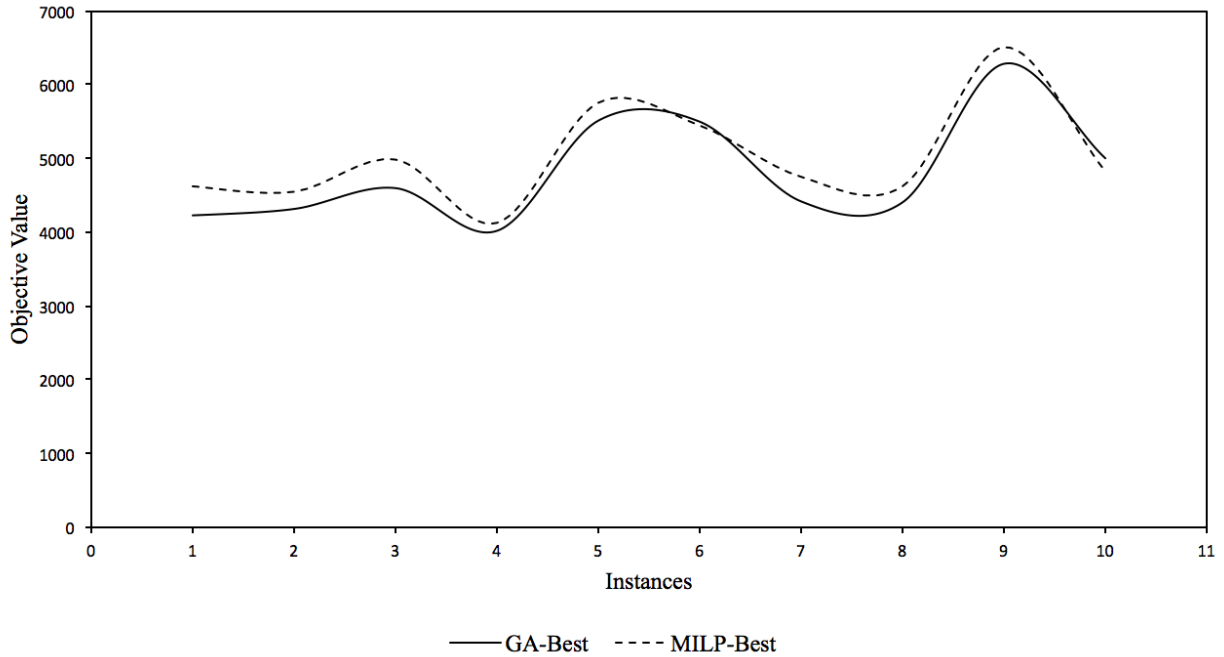


Figure 3.9: Comparison plot between GA and MILP on 30 sample size for 2 routes

3.6 Conclusion

In this chapter, we develop a mixed integer linear programming (MILP) model for solving the routing design problem for a fixed routed ridesharing service with the objective of maximizing travel demand directly served by the service. Due to the computational complexity of the MILP, a genetic algorithm based heuristic algorithm is developed to solve the problem. A case study is provided to demonstrate how the model and algorithm can be applied to generate best routes in the Manhattan area in New York City. The robustness of proposed approach is tested using a number of numerical experiments, where its performance is compared with that of the exact algorithm using CPLEX. We find that the GA based approach yields less than 10% inflation in the objective value, and that its advantage increases as the problem size increases.

Chapter 4: Conclusion and Discussion

This thesis deals with the optimal planning of fixed route ridesharing services. The first part of this thesis propose an approach for improving the profit of the service by jointly making pricing and operational (i.e., shuttle frequency) decisions. We provided an approach for estimating the demand function using publicly available data and the multinomial logit model, whose prediction accuracy of mode-choice decisions is validated using cross validation results. We then develop a nonlinear optimization model to find the optimal pricing and operating policy with the objective of maximizing expected profit. In a real-world case study of a New York City based fixed-route ridesharing service, we offer the optimal joint pricing and operational policies under varying customer awareness levels, which is expected to significantly improve the profit compared to current policy. We also find that introducing a distance-based price has only moderate influence on the total profit. Furthermore, we observe that there is an opportunity to significantly increase adoption rate of the service with little impact on profitability by adjusting the flat rate.

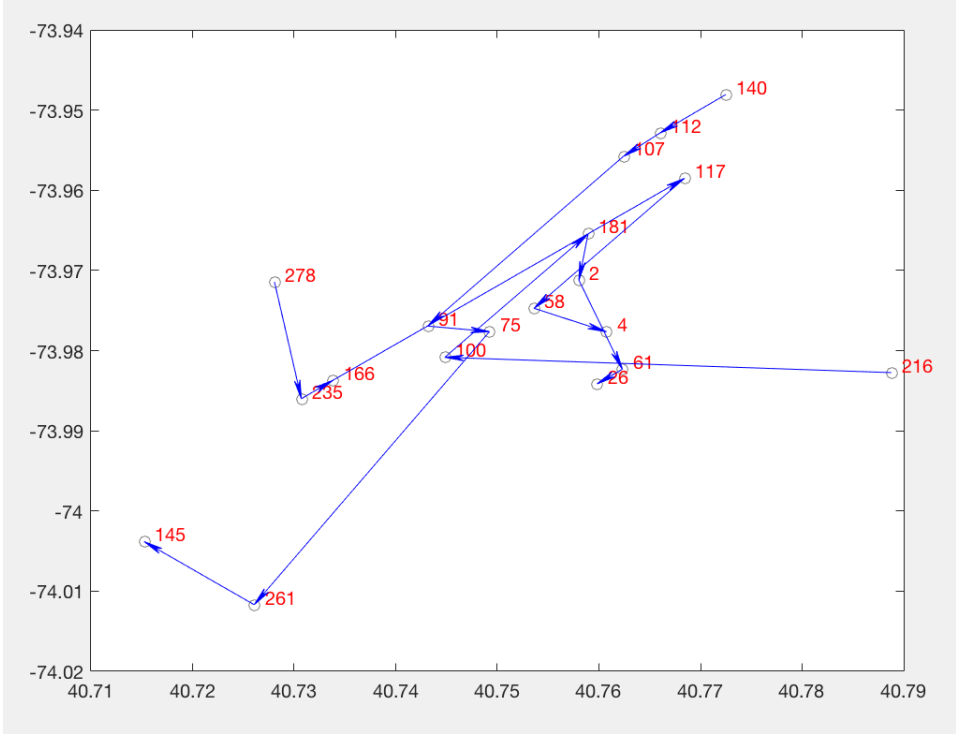
The second part of this paper discusses the routing design problem of the fixed-route ridesharing service. A mixed integer linear programming optimization (MILP) model is developed for generating the best routes that maximizes travel demand directly served. As the MILP is an NP-hard problem, a genetic algorithm based approach is proposed to generate near optimal solutions. In a Manhattan based case study, demonstrate how the model and algorithm can be applied to generate best routes. The robustness of proposed approach is tested using a

number of numerical experiments, where its performance is compared with that of the exact algorithm using CPLEX. We find that the GA based approach yields less than 10% inflation in the objective value, and that its advantage increases as the problem size increases.

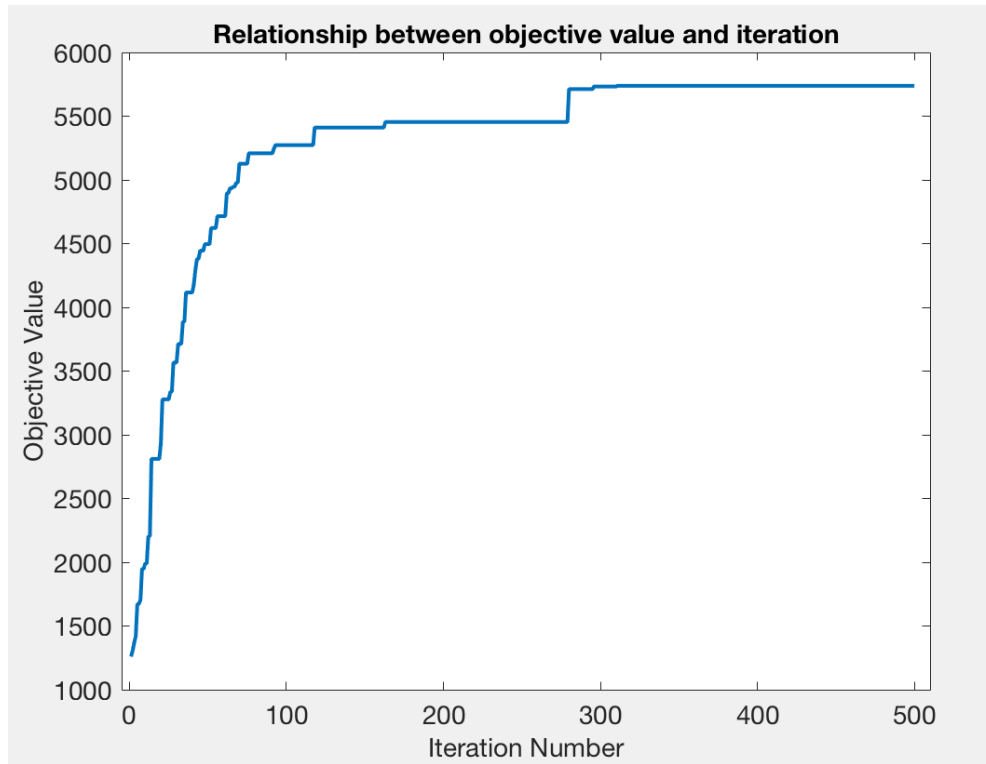
This work can be extended in several directions. First, demand of the fixed route ridesharing service is assumed to be static over time. However, in reality, the demand changes with various factors over time. The dynamic routing design and dynamic pricing can be studied if real-time demand data is available in the future. Second, there is an opportunity to combine the decisions in Chapters 2 and 3 in real world decision making. For example, decisions can be made in two stages. In the first stage, one can generate the optimal routing design. In the second stage, one can apply the pricing and operational planning model on the selected routes to maximize profitability of the service. Second stage decisions can be used as input to the first stage decision to further improve profitability. However, this is expected to substantially increase the complexity of the problem.

Appendix: Final Results of Other GA Parameter Setting

Population size: 500
Number of generations: 500

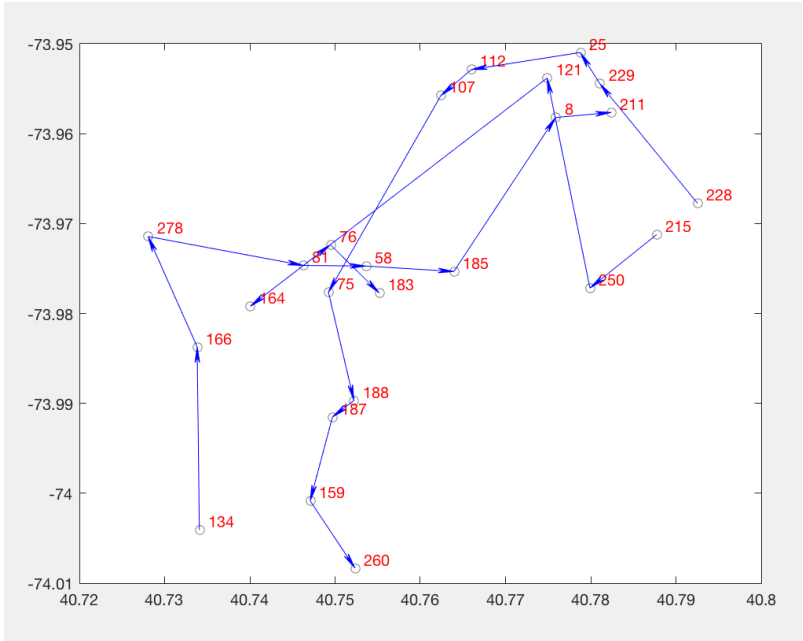


A1: Best routing design generated by GA for parameter (500, 500)

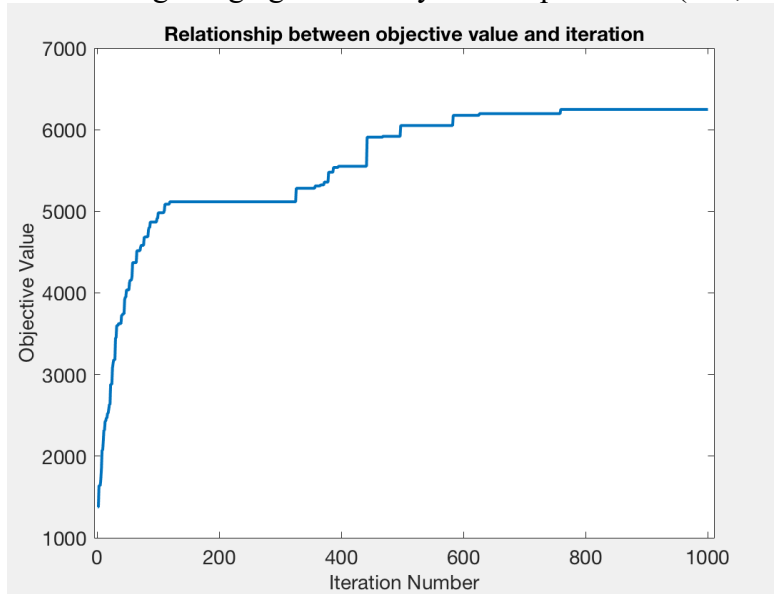


A2: GA Convergence Plot for parameter (500, 500)

Population size: 500
Number of generations: 1000

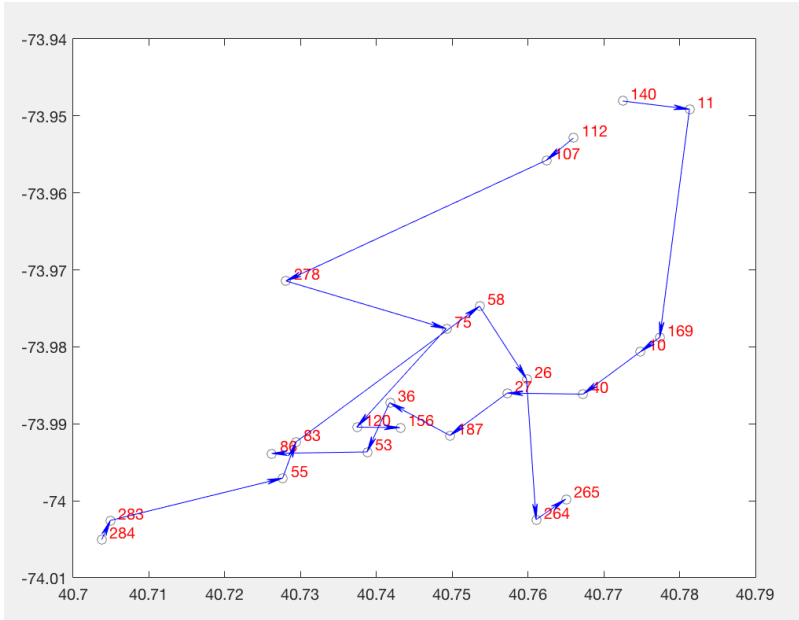


A3: Best routing design generated by GA for parameter (500, 1000)

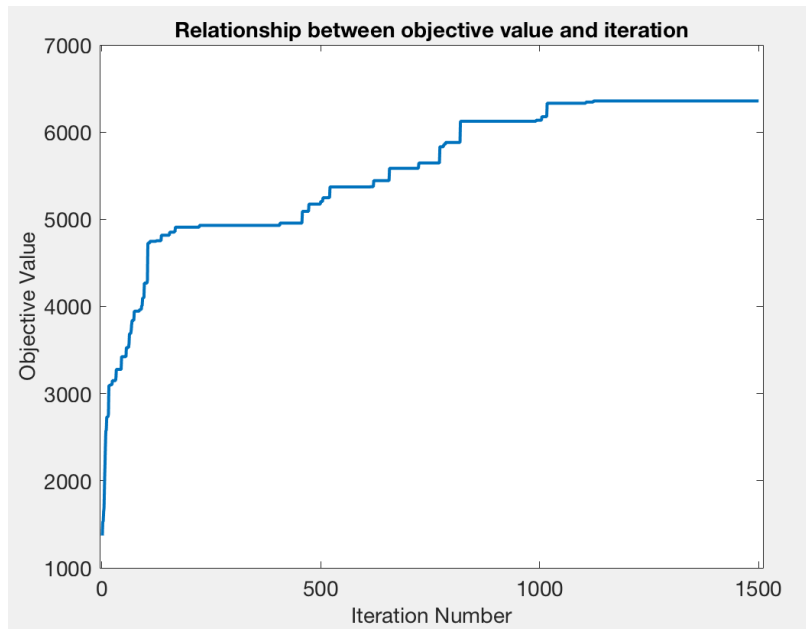


A4: GA convergence plot for parameter (500, 1000)

Population size: 500
Number of generations: 1500

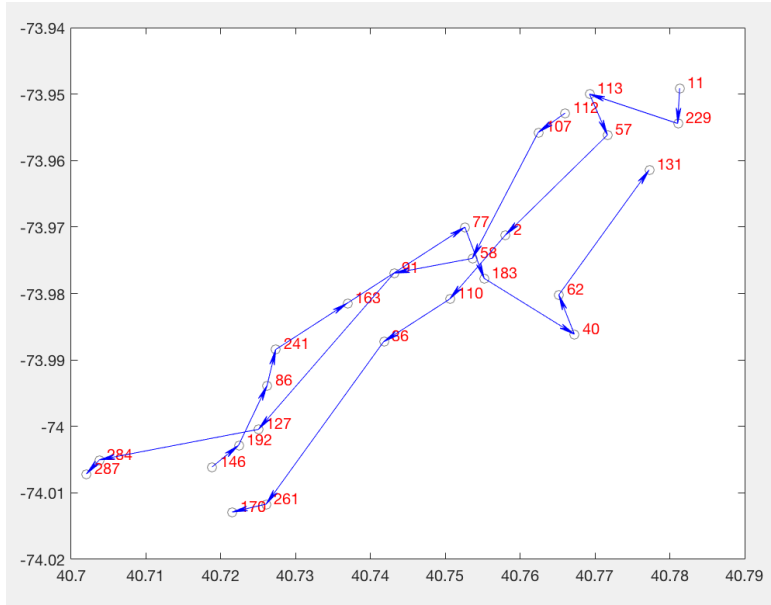


A5: Best routing design generated by GA for parameter (500, 1500)

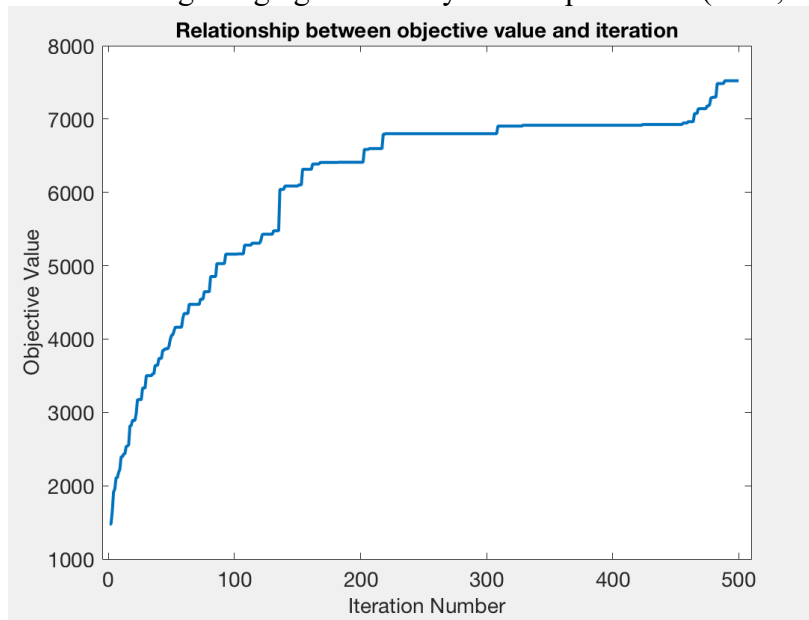


A6: GA convergence plot for parameter (500, 1500)

Population size: 1000
Number of generations: 500

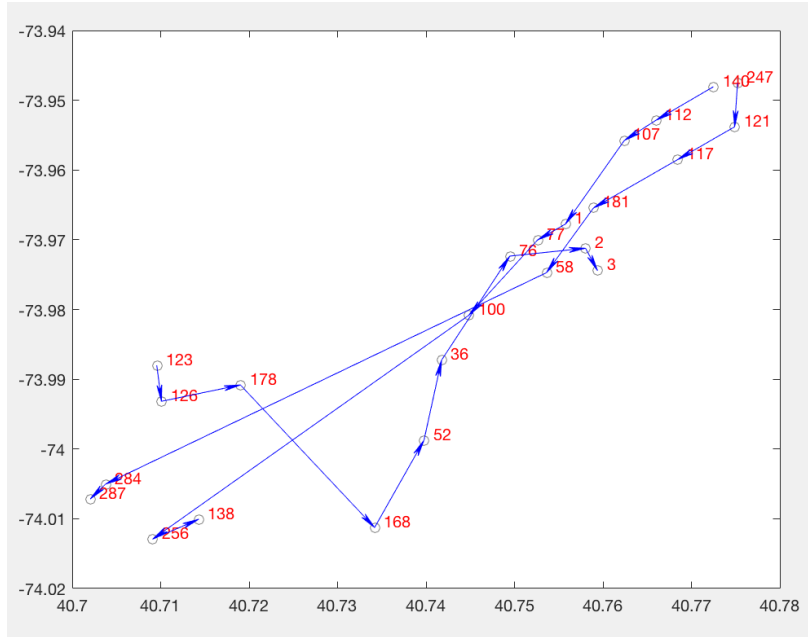


A7: Best routing design generated by GA for parameter (1000, 500)

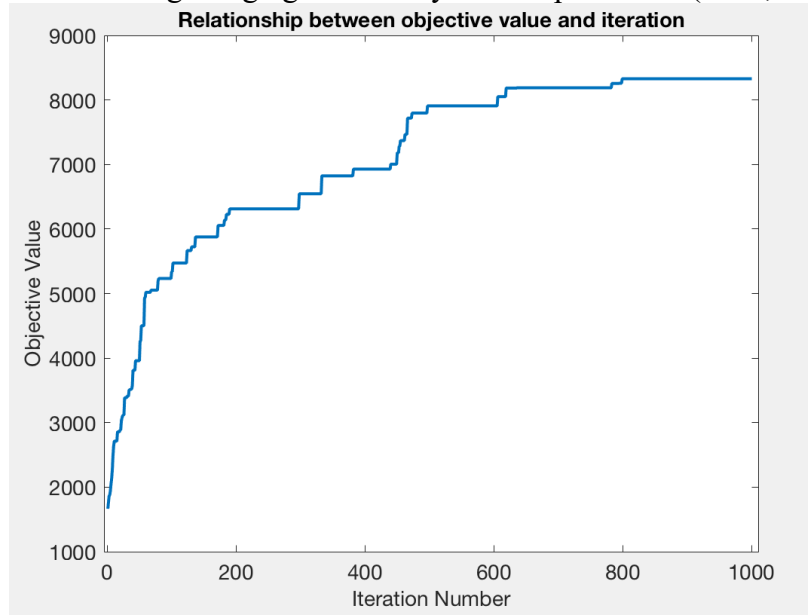


A8: GA convergence plot for parameter (1000, 500)

Population size: 1000
Number of generations: 1000



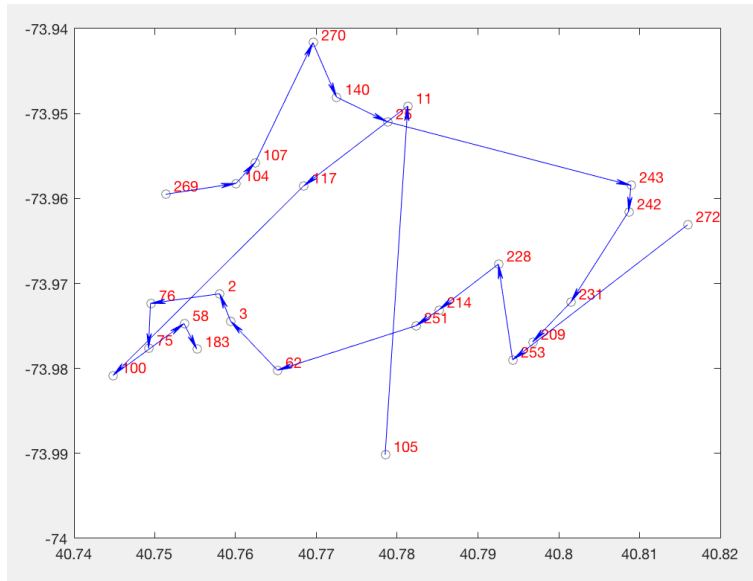
A9: Best routing design generated by GA for parameter (1000, 1000)



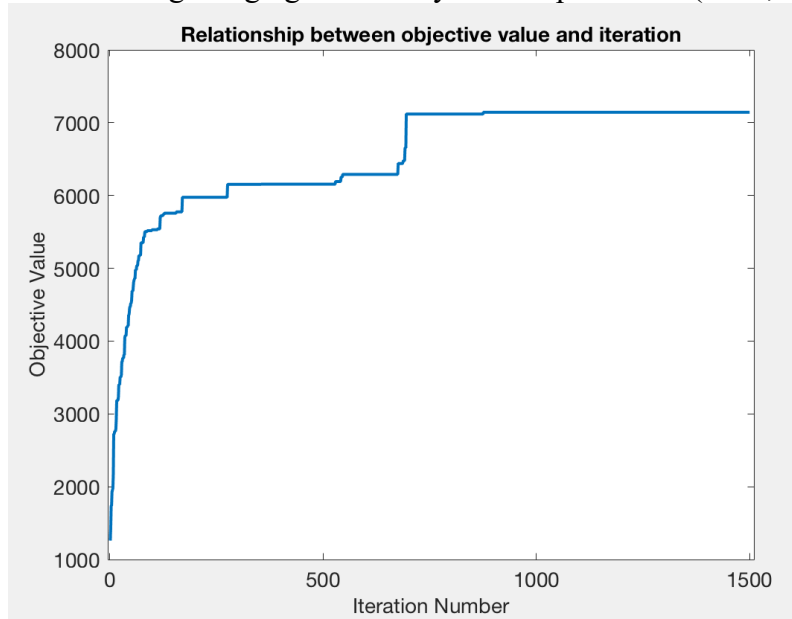
A10: GA convergence plot for parameter (1000, 1000)

Population size: 1000

Number of generations: 1500

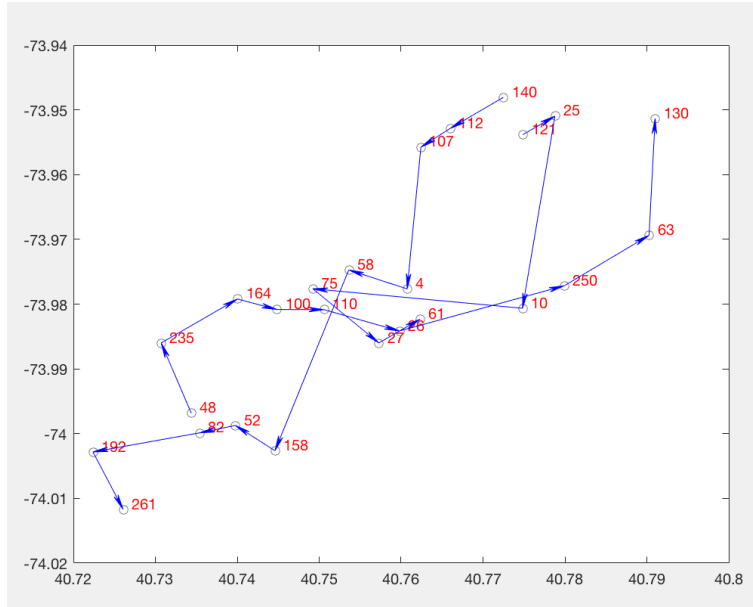


A11: Best routing design generated by GA for parameter (1000, 1500)

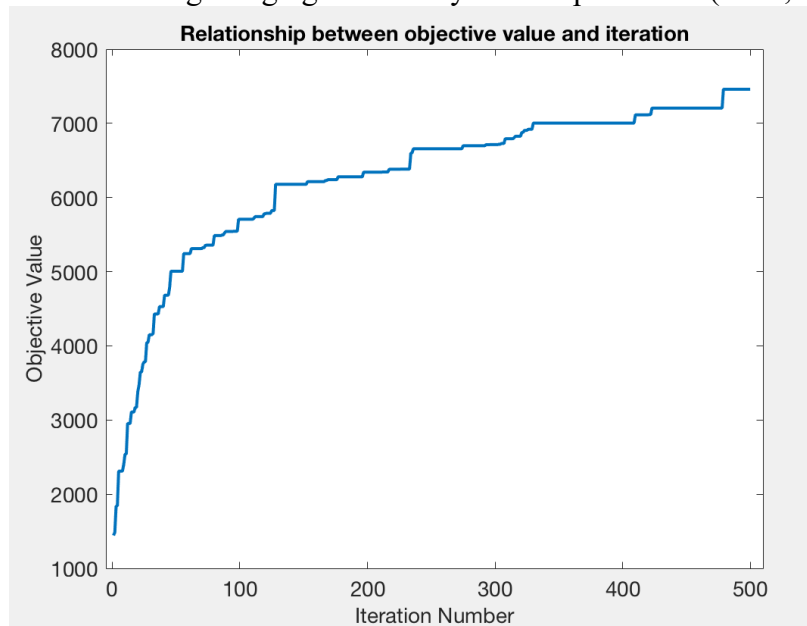


A12: GA convergence plot for parameter (1000, 1500)

Population size: 1500
Number of generations: 500



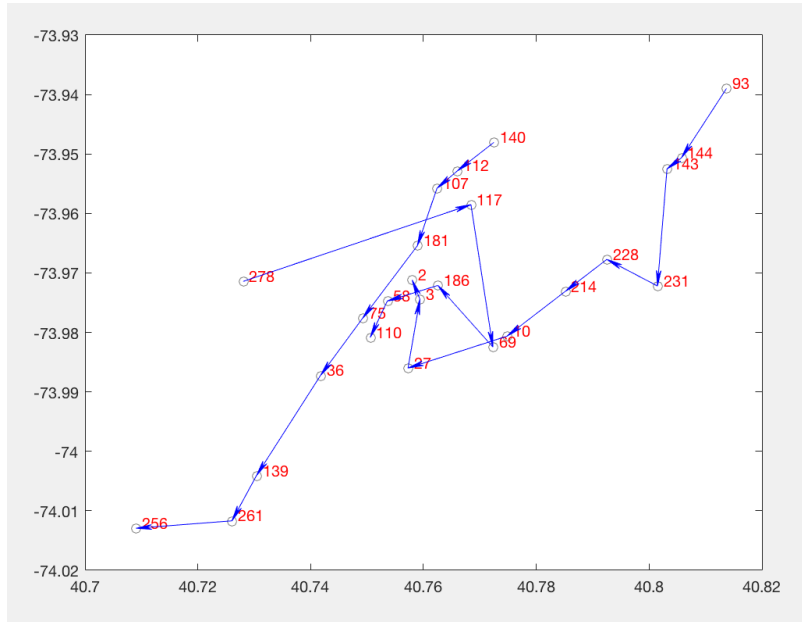
A13: Best routing design generated by GA for parameter (1500, 500)



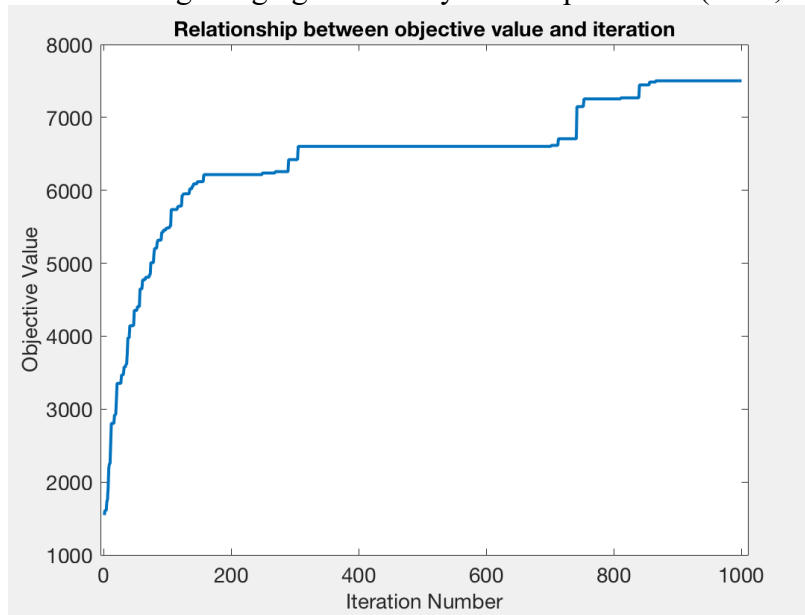
A14: GA convergence plot for parameter (1500, 500)

Population size: 1500

Number of generations: 1000



A15: Best routing design generated by GA for parameter (1500, 1000)



A16: GA convergence plot for parameter (1500, 1000)

References

- [1] Douglas, G. W. (1972). Price regulation and optimal service standards: The taxicab industry. *Journal of Transport Economics and Policy*, 116-127.
- [2] De Vany, A. S. (1975). Capacity utilization under alternative regulatory restraints: an analysis of taxi markets. *Journal of Political Economy*, 83(1), 83-94.
- [3] Arnott, R. (1996). Taxi travel should be subsidized. *Journal of Urban Economics*, 40(3), 316-333.
- [4] Chang, S. J., & Chu, C. H. (2009). Taxi vacancy rate, fare, and subsidy with maximum social willingness-to-pay under log-linear demand function. *Transportation Research Record*, 2111(1), 90-99.
- [5] Lampkin, W., & Saalmans, P. D. (1967). The design of routes, service frequencies, and schedules for a municipal bus undertaking: A case study. *Journal of the Operational Research Society*, 18(4), 375-397.
- [6] Silman, L. A., Barzily, Z., & Passy, U. (1974). Planning the route system for urban buses. *Computers & operations research*, 1(2), 201-211.
- [7] Marwah, B. R., Umrigar, F. S., & Patnaik, S. B. (1984). Optimal design of bus routes and frequencies for Ahmedabad. *Transportation Research Record*, 994, 41-47.
- [8] Nahry, S. S. (2000). Optimal scheduling of public transport fleet at network level. *Journal of advanced transportation*, 34(2), 297-323.
- [9] Lee, Y. J., & Vuchic, V. R. (2005). Transit network design with variable demand. *Journal of Transportation Engineering*, 131(1), 1-10.
- [10] Delle Site, P., & Filippi, F. (1998). Service optimization for bus corridors with short-turn strategies and variable vehicle size. *Transportation Research Part A: Policy and Practice*, 32(1), 19-38.
- [11] Chien, S. I. J., & Spasovic, L. N. (2002). Optimization of grid bus transit systems with elastic demand. *Journal of advanced transportation*, 36(1), 63-91.
- [12] Deneubourg, J. L., de Palma, A., & Kahn, D. (1979). Dynamic models of competition between transportation modes. *Environment and Planning A*, 11(6), 665-673.
- [13] Swait, J., & Ben-Akiva, M. (1987). Empirical test of a constrained choice discrete model: mode choice in Sao Paulo, Brazil. *Transportation Research Part B: Methodological*, 21(2), 103-115.
- [14] Cervero, R., & Kockelman, K. (1997). Travel demand and the 3Ds: density, diversity, and design. *Transportation Research Part D: Transport and Environment*, 2(3), 199-219.
- [15] Cervero, R. (2002). Built environments and mode choice: toward a normative framework. *Transportation Research Part D: Transport and Environment*, 7(4), 265-284.
- [16] Miller, E. J., Roorda, M. J., & Carrasco, J. A. (2005). A tour-based model of travel mode choice. *Transportation*, 32(4), 399-422.
- [17] Frank, L., Bradley, M., Kavage, S., Chapman, J., & Lawton, T. K. (2008). Urban form, travel time, and cost relationships with tour complexity and mode choice. *Transportation*, 35(1), 37-54.

- [18] Koppelman, F. S., & Bhat, C. (2006). A self instructing course in mode choice modeling: multinomial and nested logit models.
- [19] Javanmardi, M., Langerudi, M. F., Shabanpour, R., & Mohammadian, K. (2015, July). Mode choice modelling using personalized travel time and cost data. In 14th International Conference on Travel Behaviour Research.
- [20] He, L., Mak, H. Y., Rong, Y., & Shen, Z. J. M. (2017). Service region design for urban electric vehicle sharing systems. *Manufacturing & Service Operations Management*, 19(2), 309-327.
- [21] Agatz, N., Erera, A., Savelsbergh, M., & Wang, X. (2012). Optimization for dynamic ride-sharing: A review. *European Journal of Operational Research*, 223(2), 295-303.
- [22] Anderson, J. E. (2011). The gravity model. *Annu. Rev. Econ.*, 3(1), 133-160.
- [23] Yang, Y., & Diez-Roux, A. V. (2012). Walking distance by trip purpose and population subgroups. *American journal of preventive medicine*, 43(1), 11-19.
- [24] Ibarra-Rojas, O. J., Delgado, F., Giesen, R., & Muñoz, J. C. (2015). Planning, operation, and control of bus transport systems: A literature review. *Transportation Research Part B: Methodological*, 77, 38-75.
- [25] Dantzig, G., Fulkerson, R., & Johnson, S. (1954). Solution of a large-scale traveling-salesman problem. *Journal of the operations research society of America*, 2(4), 393-410.
- [26] Dantzig, G. B., & Ramser, J. H. (1959). The truck dispatching problem. *Management science*, 6(1), 80-91.
- [27] Knight, K. W., & Hofer, J. P. (1968). Vehicle scheduling with timed and connected calls: A case study. *Journal of the Operational Research Society*, 19(3), 299-310.
- [28] Pullen, H. G. M., & Webb, M. H. J. (1967). A computer application to a transport scheduling problem. *The computer journal*, 10(1), 10-13.
- [29] Golden, B. L., & Assad, A. A. (1986). OR Forum—Perspectives on Vehicle Routing: Exciting New Developments. *Operations Research*, 34(5), 803-810.
- [30] Assad, A. A. (1988). MODELING AND IMPLEMENTATION ISSUES IN VEHICLE ROUTING. *VEHICLE ROUTING: METHODS AND STUDIES. STUDIES IN MANAGEMENT SCIENCE AND SYSTEMS-VOLUME 16*.
- [31] Lenstra, J. K., Desroches, M., Savelbergh, M. W. P., & Soumis, F. (1988). Vehicle routing with time windows: optimization and approximation. *Vehicle routing: Methods and studies*, 65-84.
- [32] Dumas, Y., Desrosiers, J., & Soumis, F. (1991). The pickup and delivery problem with time windows. *European journal of operational research*, 54(1), 7-22.
- [33] Cordeau, J. F., Gendreau, M., & Laporte, G. (1997). A tabu search heuristic for periodic and multi-depot vehicle routing problems. *Networks: An International Journal*, 30(2), 105-119.
- [34] Ropke, S., & Pisinger, D. (2006). An adaptive large neighborhood search heuristic for the pickup and delivery problem with time windows. *Transportation science*, 40(4), 455-472.
- [35] Chien, S. I. J., & Spasovic, L. N. (2002). Optimization of grid bus transit systems with elastic demand. *Journal of advanced transportation*, 36(1), 63-91.
- [36] Daganzo, C. F. (2010). Structure of competitive transit networks. *Transportation Research Part B: Methodological*, 44(4), 434-446.
- [37] Fan, W., & Machemehl, R. B. (2006b). Using a simulated annealing algorithm to solve the transit route network design problem. *Journal of transportation engineering*, 132(2), 122-132.
- [38] Desrochers, M., Desrosiers, J., & Solomon, M. (1992). A new optimization algorithm for the vehicle routing problem with time windows. *Operations research*, 40(2), 342-354.

- [39] Carpaneto, G., Dell'Amico, M., Fischetti, M., & Toth, P. (1989). A branch and bound algorithm for the multiple depot vehicle scheduling problem. *Networks*, 19(5), 531-548.
- [40] Fan, W., & Machemehl, R. B. (2008). Tabu search strategies for the public transportation network optimizations with variable transit demand. *Computer-Aided Civil and Infrastructure Engineering*, 23(7), 502-520.
- [41] Fan, W., & Machemehl, R. B. (2006a). Optimal transit route network design problem with variable transit demand: genetic algorithm approach. *Journal of transportation engineering*, 132(1), 40-51.
- [42] Szeto, W., & Jiang, Y. (2012). Hybrid artificial bee colony algorithm for transit network design. *Transportation Research Record: Journal of the Transportation Research Board*, (2284), 47-56.
- [43] Chakroborty, P. (2003). Genetic algorithms for optimal urban transit network design. *Computer-Aided Civil and Infrastructure Engineering*, 18(3), 184-200.
- [44] Amiripour, S. M., Ceder, A. A., & Mohaymany, A. S. (2014). Designing large-scale bus network with seasonal variations of demand. *Transportation Research Part C: Emerging Technologies*, 48, 322-338.
- [45] Lenstra, J. K., & Kan, A. R. (1981). Complexity of vehicle routing and scheduling problems. *Networks*, 11(2), 221-227.
- [46] Wan, Q. K., & Lo, H. K. (2003). A mixed integer formulation for multiple-route transit network design. *Journal of Mathematical Modelling and Algorithms*, 2(4), 299-308.
- [47] Guan, J. F., Yang, H., & Wirasinghe, S. C. (2006). Simultaneous optimization of transit line configuration and passenger line assignment. *Transportation Research Part B: Methodological*, 40(10), 885-902.
- [48] Tasan, A. S., & Gen, M. (2012). A genetic algorithm based approach to vehicle routing problem with simultaneous pick-up and deliveries. *Computers & Industrial Engineering*, 62(3), 755-76